Journal of Computational Physics 229 (2010) 5315–5338

Contents lists available at ScienceDirect

Journal of Computational Physics

journal homepage: www.elsevier.com/locate/jcp

The influence of cell geometry on the Godunov scheme applied to the linear wave equation

Stéphane Dellacherie [a,*], Pascal Omnes [a,b], Felix Rieper [c]

[a] Commissariat à l' Énergie Atomique, CEA, DEN, DM2S-SFME, F-91191 Gif-sur-Yvette, France
[b] Université Paris 13, LAGA, CNRS UMR 7539, Institut Galilée, 99 Avenue J.-B. Clément F-93430 Villetaneuse Cedex, France
[c] Goethe-Universität Frankfurt, Institut für Atmosphäre und Umwelt, Altenhöferallee 1, D-60438 Frankfurt am Main, Germany

ARTICLE INFO

Article history:
Received 5 June 2009
Received in revised form 3 March 2010
Accepted 10 March 2010
Available online 27 March 2010

Keywords:
Compressible Euler system
Low Mach number flow
Godunov scheme
Linear wave equation
Hodge decomposition

ABSTRACT

By studying the structure of the discrete kernel of the linear acoustic operator discretized with a Godunov scheme, we clearly explain why the behaviour of the Godunov scheme applied to the linear wave equation deeply depends on the space dimension and, especially, on the type of mesh. This approach allows us to explain why, in the periodic case, the Godunov scheme applied to the resolution of the compressible Euler or Navier–Stokes system is accurate at low Mach number when the mesh is triangular or tetrahedral and is not accurate when the mesh is a 2D (or 3D) cartesian mesh. This approach confirms also the fact that a Godunov scheme remains accurate when it is modified by simply centering the discretization of the pressure gradient.

1. Introduction

In this work, we consider Godunov type schemes applied to the linear wave equation and discuss their accuracy at low Mach number, with a particular focus on the geometry (rectangular or triangular) of the underlying discretization cells. Our study was motivated by the following three facts:

1. It has long been recognized that such conservative finite-volume type schemes, like for example the Roe scheme [1] or the VFRoe scheme [2,3], are well adapted to capture shock wave solutions of the compressible Euler system but fail to correctly solve low Mach number flows. Indeed, it has been observed that when the Mach number goes to zero, Godunov type schemes create spurious pressure waves that prevent the discrete solution to be close to a discrete incompressible flow. This inaccuracy has been explained in [10,11] with formal non-linear arguments. To cure this inaccuracy, Roe type schemes modified with a Turkel's preconditioning matrix are proposed in [10–12].
2. However, it has been noticed in [21,22] that the Roe scheme remains fairly accurate on triangular meshes, and, on a very particular triangular mesh, this has been explained by graph theory arguments, still in the non-linear setting.
3. While the above-cited explanations invoked non-linear arguments, the recent work [9] has shown that this was not necessary. Indeed, at low Mach number, [9] identifies a possible source of inaccuracy generated by the Godunov scheme applied to *the linear wave equation* on rectangular meshes. It shows that an energy transfer occurs from the incompressible mode to the acoustic one, that drives the latter far away from the exact acoustic mode. Moreover, [9] has proposed a cure to this problem which consists in simply centering the discretization of the pressure gradient. The resulting new

* Corresponding author. Tel.: +33 1 69 08 15 11; fax: +33 1 69 08 10 87.
E-mail address: stephane.dellacherie@cea.fr (S. Dellacherie).

0021-9991/$ - see front matter © 2010 Elsevier Inc. All rights reserved.
doi:10.1016/j.jcp.2010.03.012

schemes have been named *low Mach X schemes* with X being any Godunov type scheme (*e.g.* $X =$ Roe or $X =$ VFRoe). Let us note that this simple modification can also be applied to any colocated X scheme that is not of Godunov type (*e.g.* $X =$ kinetic scheme [25]). Moreover, it is shown in [9] that other colocated schemes that are accurate at low Mach number [10–12,14–19] actually center or tend to center the pressure gradient when the Mach number tends to zero. Nevertheless, the theory developed in [9] is based on the notion of *first-order modified equation* which is valid on cartesian meshes but hardly generalizable to triangular meshes, and, thus, does not help in the analysis of the influence of the cell geometry on the accuracy of the scheme.

Motivated by the above three points, we have developped a theory that explains (and gives a precise meaning to) the inaccuracy at low Mach number of the Godunov scheme on cartesian meshes, the accuracy of that scheme on triangular meshes and the accuracy of the *low Mach Godunov scheme* on cartesian and triangular meshes. This theory is based on the analysis of the stationary spaces of the schemes applied to the linear wave equation and on the rate of diffusion of any numerical solution towards these spaces. For the sake of completeness, we show that our theoretical point of view also explains the accuracy of the well-known MAC scheme [26] on cartesian meshes.

Our results may be summarized as follows. Firstly, the stationary space of the Godunov scheme on rectangular cartesian meshes is a very poor subspace, unable to approach well the continuous incompressible velocity fields. Secondly, in the low Mach regime, the numerical diffusion inherent to this scheme is strong. These two facts imply that, in general, the time evolution of an initial discrete incompressible velocity field with constant pressure contains spurious acoustic modes that appear within an acoustic time scale. On the contrary, the stationary spaces of the Godunov scheme on triangular meshes, of the *low Mach Godunov scheme* on cartesian and triangular meshes and of the MAC scheme on cartesian meshes are rich enough to approach well incompressible modes and, thus, prevent the creation of spurious modes. Let us underline that a generalization of the results of [21,22] was also proposed in [13] with a formal asymptotic analysis based on powers of the Mach number. Nevertheless, this approach based on a formal asymptotic analysis, which is also used for example in [10,22], seems to us incomplete because it does not take into account the structure of the above-mentioned stationary spaces.

The outline of this article is the following. In Section 2, we recall basic results about the linear wave equation. In Section 3, we present the schemes and give a numerical illustration of their respective behaviours on a low Mach application. In Section 4, we recall the notion of first-order modified equation in the case of the linear wave equation solved with a Godunov scheme, we summarize some results proposed in [9], we describe the structure of the stationary space associated with this first-order modified equation and the time behaviour of the solution of this equation. In Section 5, we describe the stationary space and the time behaviour of the Godunov and *low Mach Godunov scheme* when the mesh is triangular or cartesian. In Section 6, we show that our point of view is compatible with the fact that a staggered scheme of MAC type [26] applied to the compressible Euler or Navier–Stokes system remains accurate at low Mach number. In Section 7, we show the connections of our theory with the approach based on a formal asymptotic analysis of the Godunov scheme [10,13,21,22]. At last, we conclude the paper in Section 8.

2. Basic results about the linear wave equation

Let us consider the (periodic) torus in $\mathbb{R}^d (d \in \{1,2,3\})$ noted $\mathbb{T}^d := [a_1, b_1] \times \cdots \times [a_d, b_d]$ and the Hilbert space $(L^2(\mathbb{T}^d))^{1+d} := \left\{ q := \begin{pmatrix} r \\ \mathbf{u} \end{pmatrix} \text{ such that } \int_{\mathbb{T}^d} r^2 dx + \int_{\mathbb{T}^d} |\mathbf{u}|^2 dx < +\infty \right\}$ equipped with the classical inner product $\langle q_1, q_2 \rangle = \int_{\mathbb{T}^d} q_1 \cdot q_2 dx$ and with the associated norm $\|q\| := \langle q, q \rangle^{1/2}$, the associated energy E being equal to $\|q\|^2$. Let us consider the linear wave equation

$$\begin{cases} \partial_t q + \dfrac{L}{M} q = 0, \\ q(t=0,x) = q^0(x), \end{cases} \tag{1}$$

where

$$Lq = a_* (\nabla \cdot \mathbf{u}, \nabla r)^T, \tag{2}$$

and $\mathbf{u} = (u, v)^T$. The quantity a_* is a strictly positive constant of order 1 and $M \ll 1$ (M is the Mach number and a_*/M is the sound velocity). The linear wave equation (1) corresponds to the linearized compressible Euler system without convection operator. The quantity $r(t,x)$ is a scaled pressure perturbation related to the pressure $p(t,x)$ through the relation

$$p(t,x) := p_* + \frac{M}{a_*} r(t,x) \tag{3}$$

(p_* is a positive constant of order 1). Let us underline that we solve linear wave equation (1) on the periodic torus $\mathbb{T}^d$ – which is equivalent to apply periodic boundary conditions – in order to lead a discussion that will not depend on the boundaries. Since $\langle q, Lq \rangle = 0$ for any q, the following well-known lemma expresses energy conservation of the wave equation:

Lemma 2.1. *The solution q of (1) is such that $\|q\|(t \geqslant 0) = \|q^0\|$.*

Let us now define the following subspaces of $(L^2(\mathbb{T}^d))^{1+d}$

$$\begin{cases} \mathcal{E} = \left\{ q := \begin{pmatrix} r \\ \mathbf{u} \end{pmatrix} \in (L^2(\mathbb{T}^d))^{1+d} \quad \text{such that } \nabla r = 0 \text{ and } \nabla \cdot \mathbf{u} = 0 \right\}, & \text{(a)} \\ \quad = \left\{ q := \begin{pmatrix} r \\ \mathbf{u} \end{pmatrix} \in (L^2(\mathbb{T}^d))^{1+d}, \quad \exists (a,b,c,\psi(\cdot)) \in \mathbb{R}^3 \times H^1(\mathbb{T}^d) \quad \text{such that } r = c \text{ and } \mathbf{u} = \begin{pmatrix} a \\ b \end{pmatrix} + \nabla \times \psi \right\}, & \text{(b)} \\ \mathcal{E}^\perp = \left\{ q := \begin{pmatrix} r \\ \mathbf{u} \end{pmatrix} \in (L^2(\mathbb{T}^d))^{1+d} \quad \text{such that } \int_{\mathbb{T}^d} r dx = 0 \text{ and } \exists \phi(\cdot) \in H^1(\mathbb{T}^d), \mathbf{u} = \nabla \phi \right\}. & \text{(c)} \end{cases} \tag{4}$$

In other words, $\mathcal{E}$ is the subspace of constant scaled pressure perturbations and incompressible velocity fields. This subset is also called *well-prepared subspace* for a reason that will be written at the end of this section. It is well-known that $(L^2(\mathbb{T}^d))^{1+d}$ may be decomposed in the following way:

Lemma 2.2

$$\mathcal{E} \oplus \mathcal{E}^\perp = (L^2(\mathbb{T}^d))^{1+d} \quad \text{and } \mathcal{E} \perp \mathcal{E}^\perp.$$

In other words, any $q \in (L^2(\mathbb{T}^d))^{1+d}$ can be decomposed into

$$q = \hat{q} + q^\perp \quad \text{where } (\hat{q}, q^\perp) \in \mathcal{E} \times \mathcal{E}^\perp, \tag{5}$$

and this decomposition – named Hodge decomposition – is unique.

In the sequel, we define the Hodge projection $\mathbb{P}$ with $\mathbb{P}q := \hat{q}$. One essential point in what follows is that

$$\mathcal{E} = KerL$$

and that, as a consequence of the linearity of L, the solution $q(t,x)$ of (1) may be decomposed as

$$q(t,x) = \mathbb{P}q^0(x) + \tilde{q}(t,x), \tag{6}$$

where $\mathbb{P}q^0$ is the Hodge projection of q^0 and $\tilde{q}$ is the solution of

$$\begin{cases} \partial_t \tilde{q} + \dfrac{L}{M} \tilde{q} = 0, \\ \tilde{q}(t=0,x) = (q^0 - \mathbb{P}q^0)(x). \end{cases} \tag{7}$$

Moreover, $\tilde{q}(t,\cdot)$ belongs to $\mathcal{E}^\perp$ for all $t \geqslant 0$, and, by energy Lemma 2.1, $\|\tilde{q}\|(t) = \|q - \mathbb{P}q\|(t=0)$. Thus, if in linear wave equation (1), the initial condition is *well-prepared* in the sense of

$$\|q - \mathbb{P}q\|(t=0) = \mathcal{O}(M), \tag{8}$$

$\tilde{q}(t,x)$ remains a perturbation of order $\mathcal{O}(M)$ at any time $t > 0$ that is to say

$$\|q - \mathbb{P}q\|(t=0) = \mathcal{O}(M) \Rightarrow \|q - \mathbb{P}q\|(t \geqslant 0) = \mathcal{O}(M). \tag{9}$$

This corresponds to a simplified version of a result by Schochet obtained in the non-linear case [20]. The fact that a given numerical scheme mimics property (9) or, on the contrary, is such that

$$\exists q^0 \in (L^2(\mathbb{T}^d))^{1+d} : \|q - \mathbb{P}q\|(t=0) = \mathcal{O}(M) \quad \text{and } \|q - \mathbb{P}q\|(\tau_{ac}) \gg \mathcal{O}(M) \tag{10}$$

(where τ_{ac} is an acoustic time scale of order M) determines the way it approaches solution of (1) at low Mach number. Relation (10) characterizes the existence of *spurious acoustic waves*. Definition (8) of *well-prepared initial condition* explains why the subspace $\mathcal{E}$ is also called *well-prepared subspace* (it is also called *incompressible subspace*). Moreover, the fact that $\mathcal{E}$ is the kernel of the acoustic operator explains why the subspace $\mathcal{E}^\perp$ is called *acoustic subspace*, $\tilde{q}(t,x)$ being a non-stationary *acoustic* wave when $(\mathbf{1} - \mathbb{P})q^0 \neq 0$. Let us underline that a standard asymptotic analysis applied to the full non-linear compressible Euler system in powers of M yields that pressure field $p(t,x)$ is the sum of a constant p_* of order 1 in space and time up to a perturbation of order M^2, and that the velocity field $\mathbf{u}(t,x)$ is the sum of an incompressible divergence-free field $\hat{\mathbf{u}}(t,x)$ plus an acoustic perturbation of order M when the initial condition is well-prepared in the sense (see for example [9] for details)

$$\begin{cases} p(t=0,x) = p_* + \mathcal{O}(M^2)(x), \\ \mathbf{u}(t=0,x) = \hat{\mathbf{u}}^0(x) + \mathcal{O}(M)(x), \end{cases} \quad \text{with } \begin{cases} p_* = C_p^{st}, \\ \nabla \cdot \hat{\mathbf{u}}^0 = 0 \end{cases} \tag{11}$$

(C_p^{st} is a positive constant of order 1; $\|\hat{\mathbf{u}}^0\|$ is also of order 1). Since $r(t,x)$ and $p(t,x)$ are linked through relation (3), we see that (8) and (11) are formally equivalent. In the same way, we easily verify that (10) – which characterizes the existence of *spurious acoustic waves* – is formally equivalent to

$$\begin{cases} p(\tau_{ac},x) = p_* + \mathcal{O}(M)(x), \\ \mathbf{u}(\tau_{ac},x) = \hat{\mathbf{u}}(\tau_{ac},x) + \mathbf{u}^\perp(\tau_{ac},x), \end{cases} \quad \text{with } \begin{cases} p_* = C_p^{st}, \\ \nabla \cdot \hat{\mathbf{u}} = 0 \quad \text{and } \|\mathbf{u}^\perp\| = \mathcal{O}(1). \end{cases} \tag{12}$$

3. The numerical schemes and their behaviours on a low Mach application

We now study with numerical experiments if (9) or (10) is verified at the discrete level when linear wave equation (1) is discretized with the Godunov scheme, with the *low Mach Godunov scheme* proposed in [9] and with the MAC scheme [26]. We recall that we apply to linear wave equation (1) periodic boundary conditions in order to lead a discussion that will not depend on the boundaries. Before showing numerical results, we firstly recall the derivation of these three schemes and, secondly, we construct a discrete version of the well-prepared subspace $\mathcal{E}$ (defined with (4)(b) in the continuous case) when the mesh is a colocated triangular mesh, a colocated cartesian mesh and a staggered cartesian mesh.

In the case of the cell-centered Godunov scheme or *low Mach Godunov scheme*, the computational domain is discretized by cells T_i which are triangular or quadrangular. Let A_{ij} be the common edge of two neighboring cells T_i and T_j, and $\mathbf{n}_{ij}$ the normal unit vector to A_{ij} pointing from T_i to T_j (note that $\mathbf{n}_{ij} = -\mathbf{n}_{ji}$). We shall denote by $|T_i|$ the area of T_i and $|A_{ij}|$ the length of A_{ij}. In the case of the *staggered* MAC scheme, the computational domain is discretized with quadrangular cells in such a way the discrete velocity field $\mathbf{u} := (u, v)^T$ is defined at the cell interface $(i+1/2, j)$ for u and at the cell interface $(i, j+1/2)$ for v, the scaled pressure r being defined at the center of the quadrangular cell (i,j). Thus, in the case of the MAC scheme, the discrete field is defined on a *staggered* cartesian mesh which is not the case for Godunov type schemes that are *colocated* schemes. In each case, the time interval of the simulation is divided into time steps Δt and n is the time subscript.

3.1. The Godunov scheme

System (1) may be written under the following form

$$\partial_t q + \partial_x(A_x q) + \partial_y(A_y q) = 0, \tag{13}$$

with

$$q = \begin{pmatrix} r \\ u \\ v \end{pmatrix}, \quad A_x = \frac{a_*}{M}\begin{pmatrix} 0 & 1 & 0 \\ 1 & 0 & 0 \\ 0 & 0 & 0 \end{pmatrix} \quad \text{and } A_y = \frac{a_*}{M}\begin{pmatrix} 0 & 0 & 1 \\ 0 & 0 & 0 \\ 1 & 0 & 0 \end{pmatrix}.$$

The one-dimensional Riemann problem associated to this equation is

$$\begin{cases} \partial_t q + \partial_\xi(A_\xi(\mathbf{n})q) = 0, \\ q(t=0,\xi) = \begin{cases} q^L & \text{if } \xi < 0, \\ q^R & \text{if } \xi > 0, \end{cases} \end{cases} \tag{14}$$

with

$$A_\xi(\mathbf{n}) = \frac{a_*}{M}\begin{pmatrix} 0 & n_x & n_y \\ n_x & 0 & 0 \\ n_y & 0 & 0 \end{pmatrix}.$$

The eigenvalues λ and associated eigenvectors $(r_\lambda, u_\lambda, v_\lambda)^T$ of A_ξ verify

$$n_x \frac{a_*}{M} r_\lambda = \lambda u_\lambda, \quad n_y \frac{a_*}{M} r_\lambda = \lambda v_\lambda \quad \text{and } n_x u_\lambda + n_y v_\lambda = \frac{M}{a_*}\lambda r_\lambda.$$

Since $n_x^2 + n_y^2 = 1$, the above equations imply that

$$\frac{a_*}{M} r_\lambda = \lambda(n_x u_\lambda + n_y v_\lambda) = \frac{M}{a_*}\lambda^2 r_\lambda.$$

Therefore, $r_\lambda = 0$ or $\lambda = \pm\frac{a_*}{M}$. If $r_\lambda = 0$, since u_λ and v_λ cannot vanish at the same time, we necessarily have $\lambda = 0$ which implies $n_x u_\lambda + n_y v_\lambda = 0$. An associated unit eigenvector is therefore

$$(r_0, u_0, v_0)^T = (0, -n_y, n_x)^T.$$

If $\lambda = -\frac{a_*}{M}$, then an associated unit eigenvector is

$$\left(r_{-\frac{a_*}{M}}, u_{-\frac{a_*}{M}}, v_{-\frac{a_*}{M}}\right)^T = \gamma(1, -n_x, -n_y),$$

with $\gamma^2 = \frac{1}{2}$. On the other hand, if $\lambda = \frac{a_*}{M}$, then an associated unit eigenvector is

$$\left(r_{\frac{a_*}{M}}, u_{\frac{a_*}{M}}, v_{\frac{a_*}{M}}\right)^T = \gamma(1, n_x, n_y)^T.$$

Now, let P be the eigenvector matrix

$$P := \begin{pmatrix} 0 & \gamma & \gamma \\ -n_y & -\gamma n_x & \gamma n_x \\ n_x & -\gamma n_y & \gamma n_y \end{pmatrix}.$$

There holds

$$P^{-1} = \begin{pmatrix} 0 & -n_y & n_x \\ (2\gamma)^{-1} & -(2\gamma)^{-1} n_x & -(2\gamma)^{-1} n_y \\ (2\gamma)^{-1} & (2\gamma)^{-1} n_x & (2\gamma)^{-1} n_y \end{pmatrix}.$$

Then, it can be checked that

$$\Lambda := P^{-1} A_\xi P = \frac{a_*}{M} \begin{pmatrix} 0 & 0 & 0 \\ 0 & -1 & 0 \\ 0 & 0 & 1 \end{pmatrix}.$$

Then, setting $w := (w_1, w_2, w_3)^T = P^{-1} q$, system (14) may be rewritten as

$$\begin{cases} \partial_t w + \partial_\xi(\Lambda w) = 0, \\ w(t=0,\xi) = \begin{cases} w^L & \text{if } \xi < 0, \\ w^R & \text{if } \xi > 0. \end{cases} \end{cases} \tag{15}$$

Now, the solution of (15) is obvious since Λ is diagonal. It is given by

$$w^{RP} := w(t, \xi = 0) = (\bar{w}_1, w_2^R, w_3^L)^T,$$

where we shall see that the exact value of $\bar{w}_1$ as a combination of w_1^R and w_1^L does not play any role in the final expression of the scheme. The expression of w^{RP} in terms of q^L and q^R is

$$w^{RP} = \begin{pmatrix} -n_y \bar{u} + n_x \bar{v} \\ -(2\gamma)^{-1}\left(n_x u^R + n_y v^R - r^R\right) \\ (2\gamma)^{-1}\left(n_x u^L + n_y v^L + r^L\right) \end{pmatrix}.$$

Therefore, the solution $q^{RP} := q(t, \xi = 0)$ is expressed by

$$q^{RP} = \begin{pmatrix} \frac{1}{2}\left[(\mathbf{u}^L - \mathbf{u}^R)\cdot\mathbf{n} + (r^L + r^R)\right] \\ n_y^2 \bar{u} - n_y n_x \bar{v} + \frac{n_x}{2}\left[(\mathbf{u}^L + \mathbf{u}^R)\cdot\mathbf{n} + (r^L - r^R)\right] \\ -n_y n_x \bar{u} + n_x^2 \bar{v} + \frac{n_y}{2}\left[(\mathbf{u}^L + \mathbf{u}^R)\cdot\mathbf{n} + (r^L - r^R)\right] \end{pmatrix}.$$

Finally, integrating (13) over the space–time domain $T_i \times [t^n, t^{n+1}]$ and applying the Gauss law yields

$$q_i^{n+1} - q_i^n + \frac{\Delta t}{|T_i|} \sum_{A_{ij} \subset \partial T_i} |A_{ij}| A_\xi(\mathbf{n}_{ij}) q_{ij}^{n+1/2} = 0,$$

where q_i^n is the averaged value of q over T_i at time t^n and $q_{ij}^{n+1/2}$ is the average value of q over $A_{ij} \times [t^n, t^{n+1}]$. In the numerical approximation, this (unknown) value of $q_{ij}^{n+1/2}$ is replaced by q^{RP} with $q^L = q_i^n$ and $q^R = q_j^n$. With the fact that

$$A_\xi(\mathbf{n}_{ij}) q^{RP} = \frac{a_*}{2M} \begin{pmatrix} (\mathbf{u}^L + \mathbf{u}^R)\cdot\mathbf{n} + (r^L - r^R) \\ n_x\left[(\mathbf{u}^L - \mathbf{u}^R)\cdot\mathbf{n} + (r^L + r^R)\right] \\ n_y\left[(\mathbf{u}^L - \mathbf{u}^R)\cdot\mathbf{n} + (r^L + r^R)\right] \end{pmatrix},$$

there finally holds

$$\begin{cases} r_i^{n+1} - r_i^n + \dfrac{a_* \Delta t}{2M|T_i|} \displaystyle\sum_{A_{ij} \subset \partial T_i} |A_{ij}| \Big[(\mathbf{u}_i^n + \mathbf{u}_j^n)\cdot\mathbf{n}_{ij} + (r_i^n - r_j^n) \Big] = 0, & \text{(a)} \\ \mathbf{u}_i^{n+1} - \mathbf{u}_i^n + \dfrac{a_* \Delta t}{2M|T_i|} \displaystyle\sum_{A_{ij} \subset \partial T_i} |A_{ij}| \Big[(r_i^n + r_j^n) + (\mathbf{u}_i^n - \mathbf{u}_j^n)\cdot\mathbf{n}_{ij} \Big] \mathbf{n}_{ij} = 0. & \text{(b)} \end{cases} \tag{16}$$

3.2. The low Mach Godunov scheme

The *low Mach Godunov scheme* [9] is deduced from Godunov scheme (16) by simply centering the pressure gradient. Thus, it is defined with

$$\begin{cases} r_i^{n+1} - r_i^n + \dfrac{a_*\Delta t}{2M|T_i|}\displaystyle\sum_{A_{ij}\subset\partial T_i} |A_{ij}|\Big[(\mathbf{u}_i^n + \mathbf{u}_j^n)\cdot\mathbf{n}_{ij} + (r_i^n - r_j^n)\Big] = 0, & \text{(a)} \\ \mathbf{u}_i^{n+1} - \mathbf{u}_i^n + \dfrac{a_*\Delta t}{2M|T_i|}\displaystyle\sum_{A_{ij}\subset\partial T_i} |A_{ij}|(r_i^n + r_j^n)\mathbf{n}_{ij} = 0. & \text{(b)} \end{cases} \tag{17}$$

In [9], a 1D Fourier analysis shows that (17) satisfies the von Neumann necessary condition for L^2 stability under a classical Courant–Friedrich–Levy (CFL) criterion.

3.3. The MAC scheme

The explicit MAC scheme applied to linear wave equation (1) is given by [27]

$$\begin{cases} r_{i,j}^{n+1} - r_{i,j}^n + \dfrac{a_*\Delta t}{M}\left(\dfrac{u_{i+1/2,j} - u_{i-1/2,j}}{\Delta x} + \dfrac{v_{i,j+1/2} - v_{i,j-1/2}}{\Delta y}\right) = 0, \\ u_{i+1/2,j}^{n+1} - u_{i+1/2,j}^n + \dfrac{a_*\Delta t}{M}\cdot\dfrac{r_{i+1,j} - r_{i,j}}{\Delta x} = 0, \\ v_{i,j+1/2}^{n+1} - v_{i,j+1/2}^n + \dfrac{a_*\Delta t}{M}\cdot\dfrac{r_{i,j+1} - r_{i,j}}{\Delta y} = 0. \end{cases} \tag{18}$$

3.4. Construction of discrete well-prepared subspaces

We now construct accurate discrete versions of the well-prepared subspace $\mathcal{E}$ (defined with (4)(b) in the continuous case) for three different meshes. In the sequel, vectors of these discrete subspaces are named *discrete incompressible fields*. The construction of these discrete subspaces are deduced from three discrete versions of the Hodge decompostion defined in Lemma 2.2 in the continuous case.

3.4.1. The colocated triangular mesh case

Let us suppose that all T_i are triangles arranged so that the computational domain is periodic. Moreover, let us denote by V_h the standard P^1 (first-order polynomial functions) Lagrange finite element space associated with this triangular mesh

$$V_h := \{\psi_h \in C_0(\overline{\mathbb{T}^d}), \psi_h \text{ periodic on } \overline{\mathbb{T}^d} \quad \text{such that } \forall T_i:\ (\psi_h)_{|T_i} \in P^1(T_i)\}. \tag{19}$$

Let us also denote by W_h the nonconforming Crouzeix–Raviart P^1 finite element space [5] associated with this triangular mesh

$$W_h := \{\phi_h \in L^2(\mathbb{T}^d), \phi_h \quad \text{periodic on } \overline{\mathbb{T}^d} \quad \text{such that } \forall T_i:\ (\phi_h)_{|T_i} \in P^1(T_i) \quad \text{and } \phi_h \quad \text{is continuous at the edge midpoints}\}.$$

Note that since the functions in V_h (resp. W_h) are P^1 on each cell, their curls (resp. their gradients) are constant vectors on each cell. Let us also define the discrete vector subspace

$$\mathcal{E}_h^A = \left\{ q := \begin{pmatrix} r \\ \mathbf{u} \end{pmatrix} \in \mathbb{R}^{3N} \quad \text{such that } \exists (a,b,c,\psi_h) \in \mathbb{R}^3 \times V_h \quad \text{such that } \forall T_i:\ r_i = c \quad \textit{and } \mathbf{u}_i = \begin{pmatrix} a \\ b \end{pmatrix} + (\nabla\times\psi_h)_{|T_i} \right\}. \tag{20}$$

Then, adapting the proof of theorem 4.1 in [6] to the case of periodic elements in V_h and W_h, we may prove the following lemma, where orthogonality is to be understood with respect to the discrete scalar product in $\mathbb{R}^{3N}$, weighted by the areas $|T_i|$:

Lemma 3.1

$$(\mathcal{E}_h^A)^\perp = \left\{ q := \begin{pmatrix} r \\ \mathbf{u} \end{pmatrix} \in \mathbb{R}^{3N} \quad \textit{such that} \quad \sum_i |T_i| r_i = 0 \textit{ and } \exists \phi_h \in W_h \quad \textit{such that } \forall T_i:\ \mathbf{u}_i = (\nabla\phi_h)_{|T_i} \right\}.$$

In other words, any $\begin{pmatrix} r \\ \mathbf{u} \end{pmatrix} \in \mathbb{R}^{3N}$ *admits the following orthogonal decomposition*

$$\begin{pmatrix} r \\ \mathbf{u} \end{pmatrix} = \begin{pmatrix} \bar r \\ \bar{\mathbf{u}} + \nabla\times\psi_h \end{pmatrix} + \begin{pmatrix} r - \bar r \\ \nabla\phi_h \end{pmatrix}, \tag{21}$$

with $\bar r = \dfrac{\sum_i |T_i| r_i}{\sum_i |T_i|}$, $\bar{\mathbf{u}} = \dfrac{\sum_i |T_i| \mathbf{u}_i}{\sum_i |T_i|}$, *and where* $(\psi_h, \phi_h) \in V_h \times W_h$.

The first element in the right hand side of (21) defines the orthogonal projection $\mathbb{P}_{\mathcal{E}_h^A} q$ of any $q = (r, \mathbf{u})^T \in \mathbb{R}^{3N}$ onto $\mathcal{E}_h^A$. The subspace $\mathcal{E}_h^A$ is a good approximation of $\mathcal{E}$ on a triangular mesh since standard approximation results show that the curls of functions in V_h approach well enough the continuous curls. More precisely, for $q := (r := c,\ \mathbf{u} := (a,b)^T + \nabla\times\psi)^T \in \mathcal{E}$, let us

define the Lagrange interpolation $\psi_h^L \in V_h$ of ψ on the triangular mesh. Then, the discretization q_h of $q \in \mathcal{E}$ on the triangular mesh given by

$$q_h := \begin{pmatrix} r_i \\ \mathbf{u}_i \end{pmatrix} \quad \text{where} \quad \left\{ \begin{array}{c} r_i = c, \\ \mathbf{u}_i = \begin{pmatrix} a \\ b \end{pmatrix} + (\nabla \times \psi_h^L)_{|T_i} \end{array} \right. \tag{22}$$

defines a discrete field that belongs to $\mathcal{E}_h^A$ and that approaches $q(B_i)$ at the order one in h if ψ is regular enough, B_i being the barycenter of the triangular cell T_i.

3.4.2. The colocated cartesian mesh case

Let us now suppose that the computational domain is a rectangle and that the mesh is made up of $N_x \times N_y$ rectangles of constant size $\Delta x \times \Delta y$ where N_x and N_y are the numbers of cells in the x and y directions. In what follows, we shall suppose that both N_x and N_y are odd. Indeed, if this is not the case, the situation is a little more involved due to even/odd decoupling which may produce checkerboard modes. Let us now define the subspace

$$\mathcal{E}_h^{\square} = \left\{ q := \begin{pmatrix} r \\ \mathbf{u} \end{pmatrix} \in \mathbb{R}^{3N_xN_y} \quad \text{such that } \exists (a,b,c,(\psi_{ij})) \in \mathbb{R}^3 \times \mathbb{R}^{N_xN_y} \quad \text{such that } \forall (i,j) : r_{ij} = c \quad \text{and } \mathbf{u}_{ij} = \begin{pmatrix} a \\ b \end{pmatrix} + \begin{pmatrix} \dfrac{\psi_{ij+1} - \psi_{ij-1}}{2\Delta y} \\ -\dfrac{\psi_{i+1j} - \psi_{i-1j}}{2\Delta x} \end{pmatrix} \right\}. \tag{23}$$

In (23), it is implicitly meant that (ψ_{ij}) is periodic that is to say:

$$\psi_{i,0} = \psi_{i,N_y} \quad \psi_{i,N_y+1} = \psi_{i,1} \quad \forall i \in [1, N_x],$$

and

$$\psi_{0,j} = \psi_{N_x,j} \quad \psi_{N_x+1,j} = \psi_{1,j} \quad \forall j \in [1, N_y].$$

The following lemma holds:

Lemma 3.2

$$(\mathcal{E}_h^{\square})^{\perp} = \left\{ q := \begin{pmatrix} r \\ \mathbf{u} \end{pmatrix} \in \mathbb{R}^{3N_xN_y} \quad \textit{such that} \quad \sum_{(ij)} r_{ij} = 0 \quad \textit{and } \exists (\phi_{ij}) \in \mathbb{R}^{N_xN_y} \quad \textit{such that } \mathbf{u}_{ij} = \begin{pmatrix} \dfrac{\phi_{i+1j} - \phi_{i-1j}}{2\Delta x} \\ \dfrac{\phi_{ij+1} - \phi_{ij-1}}{2\Delta y} \end{pmatrix} \right\}. \tag{24}$$

In other words, any $\begin{pmatrix} r \\ \mathbf{u} \end{pmatrix} \in \mathbb{R}^{3N_xN_y}$ *admits the following orthogonal decomposition*

$$\begin{pmatrix} r \\ \mathbf{u} \end{pmatrix} = \begin{pmatrix} \bar{r} \\ \bar{\mathbf{u}} + \mathbf{C}\psi \end{pmatrix} + \begin{pmatrix} r - \bar{r} \\ \mathbf{G}\phi \end{pmatrix}, \tag{25}$$

where $\bar{r} = \dfrac{\sum_{(ij)} r_{ij}}{N_xN_y}$, $\bar{\mathbf{u}} = \dfrac{\sum_{(ij)} \mathbf{u}_{ij}}{N_xN_y}$, *and where the discrete curl* $\mathbf{C}$ *and the discrete gradient* $\mathbf{G}$ *are defined through*

$$(\mathbf{C}\psi)_{ij} = \begin{pmatrix} \dfrac{\psi_{ij+1} - \psi_{ij-1}}{2\Delta y} \\ -\dfrac{\psi_{i+1j} - \psi_{i-1j}}{2\Delta x} \end{pmatrix} \quad \textit{and} \quad (\mathbf{G}\phi)_{ij} = \begin{pmatrix} \dfrac{\phi_{i+1j} - \phi_{i-1j}}{2\Delta x} \\ \dfrac{\phi_{ij+1} - \phi_{ij-1}}{2\Delta y} \end{pmatrix}.$$

The first element in the right hand side of (25) defines the orthogonal projection $\mathbb{P}_{\mathcal{E}_h^{\square}} q$ of any $q = (r, \mathbf{u})^T \in \mathbb{R}^{3N_xN_y}$ onto $\mathcal{E}_h^{\square}$. As in the case of the discrete subspace $\mathcal{E}_h^A$ defined with (20), the discrete subspace $\mathcal{E}_h^{\square}$ is a good approximation of $\mathcal{E}$ on a cartesian mesh. Indeed, for $q := (r := c,\ \mathbf{u} := (a,b)^T + \nabla \times \psi)^T \in \mathcal{E}$, let us define $\psi_{ij} = \psi(B_{ij})$ where B_{ij} is the barycenter of the cell (i,j). Then, the discretization q_h of $q \in \mathcal{E}$ on the cartesian mesh given by

$$q_h := \begin{pmatrix} r_{ij} \\ \mathbf{u}_{ij} \end{pmatrix} \quad \text{where} \quad \left\{ \begin{array}{c} r_{ij} = c, \\ \mathbf{u}_{ij} = \begin{pmatrix} a \\ b \end{pmatrix} + \begin{pmatrix} \dfrac{\psi_{ij+1} - \psi_{ij-1}}{2\Delta y} \\ -\dfrac{\psi_{i+1j} - \psi_{i-1j}}{2\Delta x} \end{pmatrix} \end{array} \right. \tag{26}$$

defines a discrete field that belongs to $\mathcal{E}_h^{\square}$ and that approaches $q(B_{ij})$ at the order two in Δx and Δy.

3.4.3. The staggered cartesian mesh case

On the cartesian staggered mesh introduced in Section 3.3, the discrete well-prepared subspace is defined with

$$\mathcal{E}_h^{MAC,\square} = \left\{ q := \begin{pmatrix} r \\ \mathbf{u} \end{pmatrix} \in \mathbb{R}^{3N_xN_y} \quad \text{such that } \exists (a,b,c,(\psi_{i+1/2,j+1/2})) \in \mathbb{R}^3 \times \mathbb{R}^{N_xN_y} \right.$$
$$\left. \text{such that } \forall (i,j) : r_{ij} = c \quad \text{and} \quad \begin{pmatrix} u_{i+1/2,j} \\ v_{ij+1/2} \end{pmatrix} = \begin{pmatrix} a \\ b \end{pmatrix} + \begin{pmatrix} \dfrac{\psi_{i+1/2,j+1/2} - \psi_{i+1/2,j-1/2}}{\Delta y} \\ -\dfrac{\psi_{i+1/2,j+1/2} - \psi_{i-1/2,j+1/2}}{\Delta x} \end{pmatrix} \right\}, \tag{27}$$

where N_x and N_y are the number of cells in the two directions of the staggered cartesian mesh. In (27), it is implicitly meant that u,v and ψ are periodic that is to say

$$\forall i \in [1, N_x] : \begin{cases} v_{i,1/2} = v_{i,N_y+1/2}, \\ \psi_{i+1/2,1/2} = \psi_{i+1/2,N_y+1/2} \end{cases}$$

et

$$\forall j \in [1, N_y] : \begin{cases} u_{1/2,j} = u_{N_x+1/2,j}, \\ \psi_{1/2,j+1/2} = \psi_{N_x+1/2,j+1/2}. \end{cases}$$

The following lemma follows from the work of Nicolaides on the MAC scheme [7,8]:

Lemma 3.3

$$(\mathcal{E}_h^{MAC,\square})^{\perp} = \left\{ q := \begin{pmatrix} r \\ \mathbf{u} \end{pmatrix} \in \mathbb{R}^{3N_xN_y} \text{ such that } \sum_{(ij)} r_{ij} = 0 \text{ and } \exists (\phi_{ij}) \in \mathbb{R}^{N_xN_y} \text{ such that } \forall (i,j) : \begin{pmatrix} u_{i+1/2,j} \\ v_{ij+1/2} \end{pmatrix} = \begin{pmatrix} \dfrac{\phi_{i+1,j} - \phi_{ij}}{\Delta x} \\ \dfrac{\phi_{ij+1} - \phi_{ij}}{\Delta y} \end{pmatrix} \right\}.$$

In other words, any $\begin{pmatrix} r \\ \mathbf{u} \end{pmatrix} \in \mathbb{R}^{3N_xN_y}$ *admits the following orthogonal decomposition*

$$\begin{pmatrix} r \\ \mathbf{u} \end{pmatrix} = \begin{pmatrix} \bar{r} \\ \bar{\mathbf{u}} + \mathbf{C}^{MAC}\psi \end{pmatrix} + \begin{pmatrix} r - \bar{r} \\ \mathbf{G}^{MAC}\phi \end{pmatrix}, \tag{28}$$

where

$$\bar{r} = \frac{\sum_{(i,j)} r_{ij}}{N_xN_y} \quad \text{and } \bar{\mathbf{u}} = \begin{pmatrix} \dfrac{\sum_{(i,j)} u_{i+1/2,j}}{N_xN_y} \\ \dfrac{\sum_{(i,j)} v_{ij+1/2}}{N_xN_y} \end{pmatrix},$$

and where the discrete curl $\mathbf{C}^{MAC}$ *and the discrete gradient* $\mathbf{G}^{MAC}$ *are defined through*

$$\begin{pmatrix} (\mathbf{C}^{MAC}\psi)_{i+1/2,j} \\ (\mathbf{C}^{MAC}\psi)_{ij+1/2} \end{pmatrix} = \begin{pmatrix} \dfrac{\psi_{i+1/2,j+1/2} - \psi_{i+1/2,j-1/2}}{\Delta y} \\ -\dfrac{\psi_{i+1/2,j+1/2} - \psi_{i-1/2,j+1/2}}{\Delta x} \end{pmatrix},$$

and

$$\begin{pmatrix} (\mathbf{G}^{MAC}\phi)_{i+1/2,j} \\ (\mathbf{G}^{MAC}\phi)_{ij+1/2} \end{pmatrix} = \begin{pmatrix} \dfrac{\phi_{i+1,j} - \phi_{ij}}{\Delta x} \\ \dfrac{\phi_{ij+1} - \phi_{ij}}{\Delta y} \end{pmatrix}.$$

The first element in the right hand side of (28) defines the orthogonal projection $\mathbb{P}_{\mathcal{E}_h^{MAC,\square}} q$ of any $q = (r, \mathbf{u})^T \in \mathbb{R}^{3N_xN_y}$ onto $\mathcal{E}_h^{MAC,\square}$. The discrete subspace $\mathcal{E}_h^{MAC,\square}$ is a good approximation of $\mathcal{E}$ on a cartesian mesh. Indeed, for $q := (r := c,\ \mathbf{u} := (a,b)^T + \nabla \times \psi)^T \in \mathcal{E}$, let us define $\psi_{i+1/2,j+1/2} = \psi(S_{i+1/2,j+1/2})$ where $S_{i+1/2,j+1/2}$ is the upper right corner of the cell (i,j). Then, the discretization q_h of $q \in \mathcal{E}$ on the cartesian mesh given by

$$q_h := \begin{pmatrix} r_{ij} \\ u_{i+1/2,j} \\ v_{ij+1/2} \end{pmatrix} \quad \text{where} \quad \begin{cases} r_{ij} = c, \\ u_{i+1/2,j} = a + \dfrac{\psi_{i+1/2,j+1/2} - \psi_{i+1/2,j-1/2}}{\Delta y}, \\ v_{ij+1/2} = b - \dfrac{\psi_{i+1/2,j+1/2} - \psi_{i-1/2,j+1/2}}{\Delta x} \end{cases} \tag{29}$$

defines a discrete field that belongs to $\mathcal{E}_h^{MAC,\square}$ and that approaches $(r(B_{ij}), u(M_{i+1/2,j}), v(M_{ij+1/2}))^T$ at the order two in Δx and Δy, where $M_{i+1/2,j}$ (resp. $M_{ij+1/2}$) is the midpoint of the vertical right (resp. horizontal upper) boundary of cell (i,j).

3.5. Numerical results

We now solve linear wave equation (1) with Godunov scheme (16) and with *low Mach Godunov scheme* (17) on a 2D cartesian mesh (of 101×101 cells) or on a triangular mesh, and with MAC scheme (18) on a 2D cartesian mesh. Here, we consider the domain $\mathbb{T}^2 = [0, 1] \times [0, 1]$, we choose $a_* = 1$ in (2) and $M = 10^{-4}$. We consider the following initial conditions $q^0 := (r^0, \mathbf{u}^0)^T$:

$$\begin{cases} r(t=0,x,y) = 1, \\ u(t=0,x,y) = 2\sin^2(\pi x)\sin(4\pi y), \\ v(t=0,x,y) = -\sin(2\pi x)\sin^2(2\pi y). \end{cases} \tag{30}$$

Obviously, setting

$$\psi(x,y) = \frac{1}{\pi}\left[\sin^2(\pi x)\sin^2(2\pi y) - \frac{1}{4}\right],$$

there holds

$$\mathbf{u}^0 = \nabla \times \psi,$$

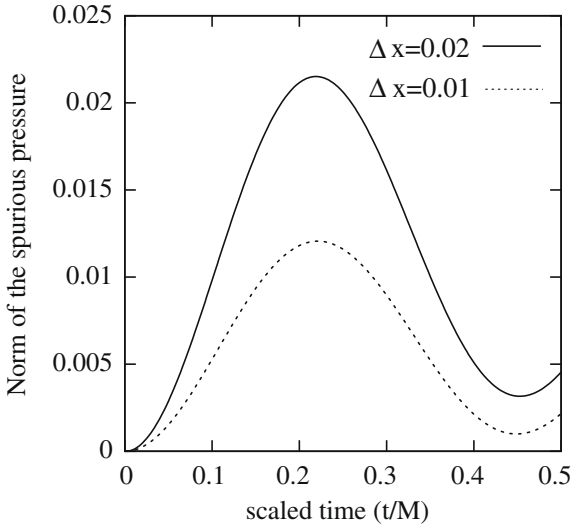

Fig. 1. Godunov scheme on a 101×101 cartesian mesh: $\|r_h^{\perp}\|(t)$.

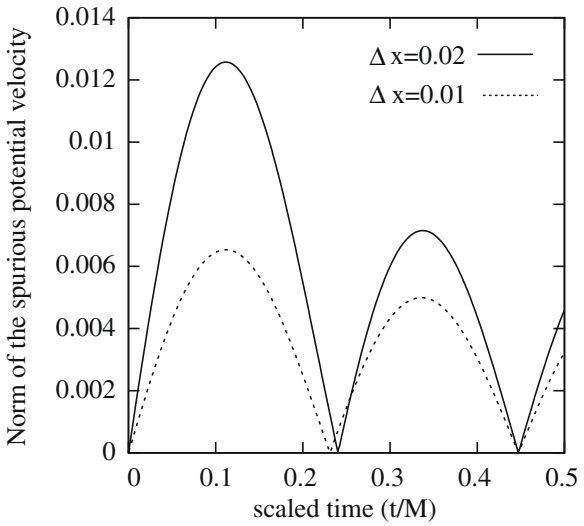

Fig. 2. Godunov scheme on a 101×101 cartesian mesh: $\|\nabla\phi_h\|(t)$.

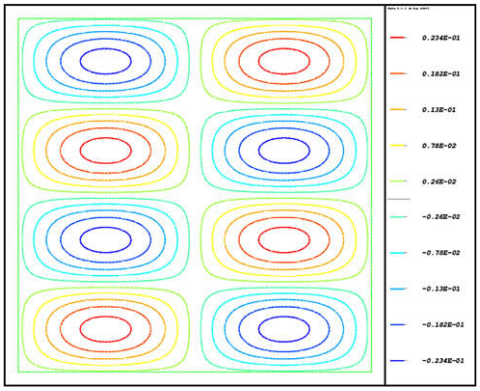

Fig. 3. Godunov scheme on a 101×101 cartesian mesh: isolines of $r_h^{\perp}(t/M = 0.15, x, y)$.

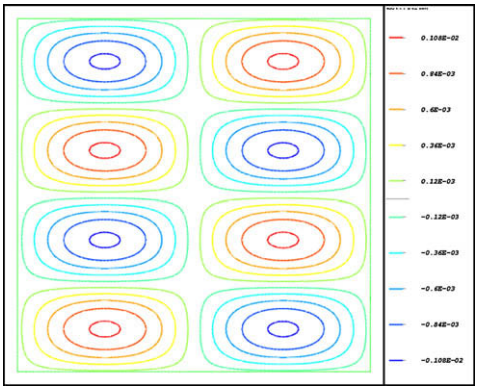

Fig. 4. Godunov scheme on a 101×101 cartesian mesh: isolines of $\phi_h(t/M = 0.15, x, y)$.

which means that, *at the continuous level*, $q^0 \in \mathcal{E}$ and, thus, that the solution of linear wave equation (1) satisfies $q(t \geqslant 0, \cdot) = q^0(\cdot)$ for initial condition (30).

Let us now discretize the initial condition q^0 on a 2D *colocated triangular mesh*, on a 2D *colocated cartesian mesh* and on a 2D *staggered cartesian mesh* by discretizing $q^0 \in \mathcal{E}$ respectively through (22) onto $\mathcal{E}_h^{\Delta}$ defined by (20), through (26) onto $\mathcal{E}_h^{\square}$ defined by (23) and through (29) onto $\mathcal{E}_h^{MAC,\square}$ defined by (27). This defines the discrete initial condition (q_h^0) for Godunov scheme (16) and for *low Mach Godunov scheme* (17), and the discrete initial condition (q_h^0) for MAC scheme (18). We also define the discrete Hodge decomposition with $\mathbb{P}_h q_h^0 := \mathbb{P}_{\mathcal{E}_h^{\Delta}} q_h^0$ in the case of the 2D *triangular mesh*, with $\mathbb{P}_h q_h^0 := \mathbb{P}_{\mathcal{E}_h^{\square}} q_h^0$ in the case of the 2D *colocated cartesian mesh* and with $\mathbb{P}_h q_h^0 := \mathbb{P}_{\mathcal{E}_h^{MAC,\square}} q_h^0$ in the case of the 2D *staggered cartesian mesh*. Thus, initial condition q_h^0 constructed from (30) is such that we have *exactly*

$$\mathbb{P}_h q_h^0 = q_h^0$$

for each mesh. This equality means that, at the discrete level, the initial condition is *well-prepared* in the sense of (8).

What we observe numerically is that in all cases, *except for the Godunov scheme on the cartesian mesh*, the numerical solutions behave exactly like in the continuous case: *they remain unchanged*. On the contrary, Figs. 1, 2 show that the numerical solution obtained with the Godunov scheme on the 2D cartesian mesh deviates from its initial value and contains a component that is in the discrete acoustic subspace $(\mathcal{E}_h^{\square})^{\perp}$ defined by (24). Indeed, defining this spurious component by $(r_h^{\perp}, \nabla\phi_h)^T := q_h - \mathbb{P}_h q_h$, we represent on Figs. 1, 2 the quantities $\|r_h^{\perp}\|(t/M)$ and $\|\nabla\phi_h\|(t/M)$ $(t/M \in [0, 0.5])$. These two figures show that

$$\|q_h - \mathbb{P}_h q_h\|(\tau_{ac}) = \mathcal{O}(\Delta x) \gg M, \tag{31}$$

where τ_{ac} is of the order of $\mathcal{O}(M)$. This estimate is the discrete version of estimate (10) and characterizes the creation of *spurious acoustic waves* at low Mach number when the linear wave equation is discretized with a standard Godunov scheme on a 2D cartesian mesh. We will justify these numerical results in Section 5 with theoretical arguments. Let us note that Figs. 3, 4 represent the isolines of $r_h^{\perp}(t/M = 0.15, x, y)$ and of $\phi_h(t/M = 0.15, x, y)$. These two figures show that $r_h^{\perp}$ and ϕ_h are deeply related.

4. Analysis of numerical schemes based on the first-order modified equation

The notion of *first-order modified equation* has been used in [9] to study the behaviour of the Godunov scheme at low Mach number applied to linear wave equation (1) on a cartesian mesh of space step Δx supposed to be identical in each direction for the sake of simplicity. Let us briefly recall this notion of first-order modified equation. When one studies the truncation error of a numerical scheme on a cartesian mesh through the use of Taylor expansions, one may add the first-order leading term of the error to the original PDE to obtain the *first-order modified equation*. For this equation, the scheme approaches the solution with a better order than for the original PDE. It is for example a well-known fact that the first-order, semi-discrete in space, upwind scheme applied to the linear transport equation $\partial_t u + a\partial_x u = 0$, with $a > 0$, is a first-order approximation of that equation, and is a second-order approximation of the first-order modified equation $\partial_t u + a\partial_x u = \frac{a}{2}\Delta x \partial^2_{xx} u$.

It was recalled in [9] that the first-order modified equation of semi-discrete in space Godunov scheme (16) and of semi-discrete in space *low Mach Godunov scheme* (17) is given by

$$\begin{cases} \partial_t q + \dfrac{L_\kappa}{M} q = 0, & \text{(a)} \\ q(t=0,x) = q^0(x), & \text{(b)} \end{cases} \tag{32}$$

with

$$\begin{cases} L_\kappa = L - MB_\kappa, \\ B_\kappa q = \mathcal{K} \begin{pmatrix} \Delta r \\ \dfrac{\partial^2 u}{\partial x^2} \\ \dfrac{\partial^2 v}{\partial y^2} \end{pmatrix} \quad \text{and } \mathcal{K} = \begin{pmatrix} v_r & 0 & 0 \\ 0 & \kappa v_u & 0 \\ 0 & 0 & \kappa v_v \end{pmatrix}, \end{cases} \tag{33}$$

where $q := (r,u,v)^T$. In (33), $(v_r, v_{\mathbf{u}}) \in \mathbb{R}^3_+ (v_{\mathbf{u}} := (v_u, v_v))$ and $v_r = v_u = v_v = v_{num} := a_* \frac{\Delta x}{2M}$ (v_{num} is the numerical viscosity) and Δr is the Laplacian operator applied to r. The case $\kappa = 1$ corresponds to the standard "full" upwind Godunov scheme (16), and the case $\kappa = 0$ corresponds to the *low Mach Godunov scheme* (17) in which the pressure gradient is centered. The 3D formulation of 2D operator (33) is similar.

4.1. Invariance of the well-prepared subspace $\mathcal{E}$

In what follows, we will say that a subspace is invariant for Eq. (32) if the solution of (32) with an initial condition in that subspace remains in that subspace for all $t > 0$. A subspace will be called stationary if the solution of (32) with an initial condition in that subspace remains equal to this initial condition for all $t > 0$.

In [9], the following lemma was proven (see lemma 4.2 in [9]):

Lemma 4.1. *We have:*

(1) when $\Omega = \mathbb{T}^{d=1}$: $\forall \kappa$, the subspace $\mathcal{E}$ is invariant for Eq. (32);
(2) when $\Omega = \mathbb{T}^{d\in\{2,3\}}$, the subspace $\mathcal{E}$ is invariant for Eq. (32) if and only if $\kappa = 0$ (low Mach Godunov scheme). Moreover, $\mathcal{E}$ is a stationary subspace when $\kappa = 0$.

We deduce from Lemma 4.1 and from the L^2 stability ($\kappa \geqslant 0$) of the solution of (32) that

$$\|q - \mathbb{P}q\|(t=0) = \mathcal{O}(M) \Rightarrow \|q - \mathbb{P}q\|(t \geqslant 0) = \mathcal{O}(M) \tag{34}$$

in dimension one when $\kappa = 1$ (Godunov scheme) or when $\kappa = 0$ (*low Mach Godunov scheme*) and, in dimension two and three, only when $\kappa = 0$ (*low Mach Godunov scheme*). Moreover, we deduce from *point 2* of Lemma 4.1 that, in dimension two or three, we can write

$$\|q - \mathbb{P}q\|(t=0) = \mathcal{O}(M) \quad \text{does not imply that } \|q - \mathbb{P}q\|(t \geqslant 0) = \mathcal{O}(M) \tag{35}$$

when $\kappa = 1$ (Godunov scheme). More precisely, when $\kappa = 1$ (Godunov scheme) and when $M \ll \Delta x$, it is also proven in [9] (see proposition 4.1 in [9]) by applying a Fourier analysis to (32) that in 2D or 3D, we have

$$\exists q^0 \in (L^2(\mathbb{T}^d))^{1+d} : \|q - \mathbb{P}q\|(t=0) = \mathcal{O}(M) \quad \text{and } \|q - \mathbb{P}q\|(\tau_{ac}) \gg \mathcal{O}(M), \tag{36}$$

where $\tau_{ac} = \mathcal{O}(\frac{ML_\Omega}{a_*})$ (τ_{ac} is an acoustic time scale, L_Ω being a characteristic length of Ω of order one). Estimate (34) means that when the initial condition is close to an incompressible flow, the solution $q(t)$ of (32) remains close to an incompressible flow at any time, just like for the linear wave equation (see (9)). Let us note that the acoustic subspace $\mathcal{E}^\perp$ is also an invariant subspace if and only if $\kappa = 0$ but this point is not important for the problem studied is this paper (note also that $\mathcal{E}^\perp$ is not a stationary subspace). Estimate (36) – which characterizes the existence of *spurious acoustic waves* – implies that the pressure

$r(\tau_{ac},x)$ has an oscillating component of order 1 and, thus, that the pressure $p(\tau_{ac},x)$ has an oscillating component of order M because of (3) (this corresponds to the creation of the well-known spurious pressure waves of order M [10,11]). It also implies that the velocity field $\mathbf{u}(\tau_{ac},x)$ has a non divergence-free component of order 1. As a consequence, at low Mach number, Godunov type schemes are accurate in 1D but are inaccurate in 2D or 3D (unless $\Delta x = \mathcal{O}(M)$ which is too restrictive for practical applications). To summarize, the inaccuracy of 2D or 3D (non-linear) Godunov type schemes can be explained when the mesh is cartesian by the fact that the well-prepared subspace $\mathcal{E}$ is not invariant for the linear first-order modified equation (32). This underlines that, when the mesh is cartesian, this inaccuracy can be explained (at least partly) with linear arguments without the convection and, thus, without the notion of shear waves[1], which implies that previous analysis proposed in [4,10–12,21,22] may be greatly simplified by dropping the convection and the non-linearities (although the papers [4,10–12,21,22] do not explicitly mention that the convection is responsible for the inaccuracy). Nevertheless, *point 2* of Lemma 4.1 shows that we recover the invariance of $\mathcal{E}$ when we impose $\kappa = 0$ in (33). This suggests that if we modify the Godunov type schemes by using a central difference to discretize the pressure gradient in the compressible Euler system, we obtain a modified Godunov type scheme that is accurate at low Mach number. Numerical results proposed in [9] justify this assertion. These modified Godunov type schemes are called *low Mach Godunov schemes*, and are defined by scheme (17) in the case of linear wave equation (1). Let us note that this simple modification can be applied to any colocated scheme and on any mesh.

Unfortunately, when the mesh is not cartesian, we cannot apply directly the previous analysis since it is difficult to generalize the notion of modified equation in that case. Nevertheless, it is possible to also link the accuracy or the inaccuracy of Godunov scheme (16) or of *low Mach Godunov scheme* (17) to the structure of the kernel $Ker\mathbb{L}_{\kappa,h}$ where $\mathbb{L}_{\kappa,h}$ is a discrete version of L_κ defined by (33) (here and in the sequel, the parameter h is the order of magnitude of the space step of the mesh). *This point of view will be adapted to explain why Godunov scheme (16) is accurate when the mesh is triangular or tetrahedral since the notion of kernel exists for any type of mesh contrary to the notion of modified equation. Moreover, in the case of a cartesian mesh, this point of view will be coherent with the analysis proposed in [9] and summarized previously*.

Before studying the discrete case, we introduce for *didactic* reasons this new point of view in the case of first-order modified Eq. (32) studied at the continuous level.

4.2. Structure of $KerL_\kappa$ and time behaviour

Another way to understand the difference between standard Godunov scheme (16) and *low Mach Godunov scheme* (17) is to study the structure of the kernel $KerL_\kappa$ and to compare the solution[2] $q_\kappa(t)$ of (32) with the solution $q(t)$ of linear wave equation (1) given by (6).

4.2.1. Structure of $KerL_\kappa$

We have the following result (see lemma 4.3 in [9]):

Lemma 4.2. *When $\Omega = \mathbb{T}^{d=2}$, we have*[3]

$$KerL_{\kappa=1} = \left\{ q := \begin{pmatrix} r \\ \mathbf{u} \end{pmatrix} \in (L^2(\mathbb{T}^2))^3 \quad \text{such that } \exists (c, u(y), v(x)) \quad \text{such that } r = c \quad \text{and } \mathbf{u} = \begin{pmatrix} u \\ v \end{pmatrix} \right\}, \tag{37}$$

which implies that

$$KerL_{\kappa=1} \subsetneq \mathcal{E}. \tag{38}$$

Moreover, we have

$$KerL_{\kappa=0} = \mathcal{E}. \tag{39}$$

Relations (37) and (38) show that $KerL_{\kappa=1}$ is a very poor subspace of $\mathcal{E}$ in two (and three) dimensions. Moreover, the subspace $KerL_{\kappa=1}$ verifies $KerL_{\kappa=1} \oplus (KerL_{\kappa=1})^\perp = (L^2(\mathbb{T}^2))^{1+d}$. Thus, we can define the orthogonal projection $\mathbb{P}_{\kappa=1} q$ of any $q \in (L^2(\mathbb{T}^2))^{1+d}$ on the stationary subspace $KerL_{\kappa=1}$ of (32). We deduce from Lemma 4.2 that:

Lemma 4.3. *When $\Omega = \mathbb{T}^{d=2}$, the projection $\mathbb{P}_{\kappa=1}$ is defined by*

$$\forall q \in (L^2(\mathbb{T}^2))^{1+d} : \mathbb{P}_{\kappa=1} q = \begin{pmatrix} \dfrac{1}{|\Omega|} \displaystyle\int_\Omega r(x,y)\,dxdy \\ \dfrac{1}{b_1 - a_1} \displaystyle\int_{a_1}^{b_1} u(x,y)\,dx \\ \dfrac{1}{b_2 - a_2} \displaystyle\int_{a_2}^{b_2} v(x,y)\,dy \end{pmatrix}.$$

[1] Let us underline that in [4] (see p. 362 in [4]), the origin of the inaccuracy is linked to a bad coupling between shear and acoustic waves.

[2] For the sake of simplicity, we now omit the spatial dependence in the notations.

[3] The result is similar when the space dimension is equal to three.

Let us underline that (see lemma 4.3 in [9]):

$$When \quad \Omega = \mathbb{T}^{d=1} : Ker L_{\kappa\in\{0,1\}} = \mathcal{E}. \tag{40}$$

The difference between (38) and (40) underlines that the behaviour of the Godunov scheme cannot be the same in dimension one and in dimension two (or three). This point is coherent with Lemma 4.1. Let us underline that (38) and the loss of invariance described in Lemma 4.1 are not identical notions. Indeed:

- strict inclusion (38) underlines that, firstly, the operator L_κ – which is a perturbation of the linear operator L – does not perturb the zero eigenvalue of L and, secondly, "shrinks" the eigenspace associated to this zero eigenvalue;
- the notion of invariance – which is not restricted to linear operators – is different from the notion of kernel since it does not suppose the existence of a zero eigenvalue. In a way, it is more general.

4.2.2. Time behaviour

We now study the time behaviour of the solution $q_\kappa(t)$ of first-order modified Eq. (32) by using the splitting

$$q_\kappa(t) = q^a_\kappa(t) + q^b_\kappa(t). \tag{41}$$

In (41), $q^a_\kappa(t)$ is solution of (32) with the initial condition

$$q^a_\kappa(t=0) = \mathbb{P}q^0, \tag{42}$$

and $q^b_\kappa(t)$ is solution of (32) with the initial condition

$$q^b_\kappa(t=0) = (\mathbf{1}-\mathbb{P})q^0. \tag{43}$$

Comparing (41) with (6), we may say that if we admit that $\|q^b_\kappa(t)\| = \mathcal{O}(M)$ when the initial condition is well-prepared that is to say when $\|q - \mathbb{P}q\|(t=0) = \mathcal{O}(M)$ (we admit that (32) is well-posed), then $q_\kappa(t)$ will or will not be a good approximation of $q(t)$ depending on the time behaviour of the quantity $q^a_\kappa(t) - \mathbb{P}q^0$. The time behaviour of $q^a_\kappa(t) - \mathbb{P}q^0$ is deeply related to the structure of $Ker L_\kappa$ and is described by the following five points:

- *Point 1:* The quantity $\|q^a_{\kappa=1}(t) - \mathbb{P}q^0\|$ is at least of order $\frac{\Delta x}{L_\Omega}\|(\mathbf{1}-\mathbb{P}_{\kappa=1})\mathbb{P}q^0\|$ as soon as t is of order $\dfrac{ML_\Omega}{a_*}$ where L_Ω is a characteristic length of order one which depends only on Ω.
- *Point 2:* The quantity $\|q^a_{\kappa=1}(t) - \mathbb{P}q^0\|$ is at least of order $\|(1-\mathbb{P}_{\kappa=1})\mathbb{P}q^0\|$ as soon as t is of order $\dfrac{ML^2_\Omega}{a_*\Delta x}$. The proof of *points 1* and *2* is given below.
- *Point 3: Behaviour of Godunov scheme in dimension two or three* ($\kappa = 1$ *and* $d \in \{2,3\}$): when the space dimension d is greater than one, $Ker L_{\kappa=1}$ is a very poor subspace of $\mathcal{E}$ (see (37) and (38)). As a consequence, $\|(1-\mathbb{P}_{\kappa=1})\mathbb{P}q^0\|$ is generally of order one. Thus, we deduce from previous *point 1* that we have generally

$$\|q^a_{\kappa=1}(t) - \mathbb{P}q^0\| \geqslant \mathcal{O}(\Delta x) \quad \text{when} \quad t = \mathcal{O}(M). \tag{44}$$

Because of this estimate, $q_{\kappa=1}(t)$ is not a good approximation of $q(t)$. Nevertheless, we cannot deduce directly from (44) estimate (36) that characterizes the creation of spurious acoustic waves in the acoustic subspace $\mathcal{E}^\perp$. Indeed, (36) is stronger than (44). Nevertheless, knowing that (36) was proven in [9], we can consider (44) as a direct consequence of the creation of spurious acoustic waves. Let us note that q^0 in (36) is the one for which $\|(1-\mathbb{P}_{\kappa=1})\mathbb{P}q^0\| = \mathcal{O}(1)$ in 2D or in 3D.

- *Point 4: Behaviour of low Mach Godunov scheme* ($\kappa = 0$ *and* $d \in \{1,2,3\}$): relation (39) implies that $\mathbb{P}_{\kappa=0} = \mathbb{P}$, which implies that

$$\forall t \geqslant 0 : q^a_{\kappa=0}(t) = \mathbb{P}q^0. \tag{45}$$

But, we have also

$$\begin{aligned}\|q_{\kappa=0}(t) - \mathbb{P}q_{\kappa=0}(t)\| &\leqslant \|q^a_{\kappa=0}(t) - \mathbb{P}q^a_{\kappa=0}(t)\| + \|q^b_{\kappa=0}(t) - \mathbb{P}q^b_{\kappa=0}(t)\| \\ &\leqslant \|q^a_{\kappa=0}(t) - \mathbb{P}q^a_{\kappa=0}(t)\| + \|q^b_{\kappa=0}(t)\| \quad (\text{since } \||1-\mathbb{P}\|| = 1),\end{aligned}$$

that is to say

$$\|q_{\kappa=0}(t) - \mathbb{P}q_{\kappa=0}(t)\| \leqslant \|q^a_{\kappa=0}(t) - \mathbb{P}q^a_{\kappa=0}(t)\| + \mathcal{O}(M), \tag{46}$$

when the initial condition is well-prepared in the sense of (8). Then, we deduce estimate (34) from (45) and (46) (since (45) implies that $q^a_{\kappa=0}(t) = \mathbb{P}q^a_{\kappa=0}(t)$). Thus, $q_{\kappa=0}(t)$ is a good approximation of $q(t)$ and no spurious acoustic waves are created by the *low Mach Godunov scheme*.

- *Point 5: Behaviour in dimension one* ($\kappa \in \{0,1\}$ *and* $d = 1$): when the space dimension d is equal to one, relation (40) implies that $\mathbb{P}_{\kappa\in\{0,1\}} = \mathbb{P}$. Then, (45) and (46) are also verified, and (34) is satisfied. Thus, $q_{\kappa=0}(t)$ is a good approximation of $q(t)$ and no spurious acoustic waves are created by the Godunov scheme ($\kappa = 1$) and by the *low Mach Godunov scheme* ($\kappa = 0$).

Points 3, *4* and *5* are coherent with the results of [9] recalled in Section 4.1. We also deduce from *points 2* and *3* that

$$\|q^a_{\kappa=1}(t) - \mathbb{P}q^0\| \geqslant \mathcal{O}(1) \quad \text{when} \quad t = \mathcal{O}\left(\frac{M}{\Delta x}\right). \tag{47}$$

This means that the long-time solution of (32) is very far from the exact solution of the original wave equation. More precisely, we will prove that $q^a_{\kappa=1}(t)$ tends to $\mathbb{P}_{\kappa=1}\mathbb{P}q^0$ when t grows (see below Proposition 4.1), $\mathbb{P}_{\kappa=1}\mathbb{P}q^0$ being generally very different from $\mathbb{P}q^0$ (see Lemma 4.3). On the other hand, when $\kappa = 0$ (*low Mach Godunov scheme*), $q^a_{\kappa=0}(t)$ remains forever exactly equal to $\mathbb{P}q^0$ (see (45)). Nevertheless, we want to emphasize that the long-time behaviour of $q_\kappa(t)$ is not really interesting when we are interested in analysing the accuracy of Godunov type schemes applied to the non-linear compressible Euler system at low Mach number. Indeed, linear wave equation (1) can be seen as a part of the linearization of the non-linear compressible Euler system at low Mach number [9]. Thus, the velocity field deduced from $q_\kappa(t)$ gives relevant information on the discrete velocity field solution of the discrete non-linear compressible Euler system only on short times of order $\mathcal{O}(M)$.

The proof of above *points 1* and *2* is a consequence of the following results:

Proposition 4.1. *When* $\kappa = 1$, *there exists a constant* L_Ω *depending only on* Ω *such that*

$$\forall t \geqslant 0 : \|q^a_{\kappa=1}(t) - \mathbb{P}_{\kappa=1}\mathbb{P}q^0\| \leqslant \|(\mathbf{1} - \mathbb{P}_{\kappa=1})\mathbb{P}q^0\| \exp\left(-\frac{a_*\Delta x}{2ML_\Omega^2}t\right). \tag{48}$$

This proposition expresses the fast diffusion of $\mathbb{P}q^0$ towards $\mathbb{P}_{\kappa=1}\mathbb{P}q^0$ when $\kappa = 1$. We deduce the following corollary from Proposition 4.1:

Corollary 4.1. *When* $\kappa = 1$, *there exists a constant* L_Ω *depending only on* Ω *such that*

$$\forall t \geqslant 0 : \|q^a_{\kappa=1}(t) - \mathbb{P}q^0\| \geqslant \left[1 - \exp\left(-\frac{a_*\Delta x}{2ML_\Omega^2}t\right)\right]\|(1 - \mathbb{P}_{\kappa=1})\mathbb{P}q^0\|. \tag{49}$$

As a consequence, we have

$$\forall t \geqslant \frac{ML_\Omega}{a_*} : \|q^a_{\kappa=1}(t) - \mathbb{P}q^0\| \geqslant \frac{\Delta x}{3L_\Omega}\|(1 - \mathbb{P}_{\kappa=1})\mathbb{P}q^0\| \tag{50}$$

for Δx *sufficiently small, and*

$$\forall t \geqslant \frac{ML_\Omega^2}{a_*\Delta x} : \|q^a_{\kappa=1}(t) - \mathbb{P}q^0\| \geqslant \left(1 - \frac{1}{\sqrt{e}}\right)\|(1 - \mathbb{P}_{\kappa=1})\mathbb{P}q^0\| \tag{51}$$

for any Δx.

The proof of Proposition 4.1 is based on the following lemma:

Lemma 4.4. *We have*

$$\forall t \geqslant 0 : \mathbb{P}_{\kappa=1}(q^a_{\kappa=1}(t) - \mathbb{P}_{\kappa=1}\mathbb{P}q^0) = 0. \tag{52}$$

It is also based on this second lemma:

Lemma 4.5. *There exists a constant* L_Ω *depending only on* Ω *such that*

$$\forall t \geqslant 0 : \|q(t)\|^2 \leqslant L_\Omega^2(\|\nabla r(t)\|^2_{L^2(\Omega)} + \|\partial_x u(t)\|^2_{L^2(\Omega)} + \|\partial_y v(t)\|^2_{L^2(\Omega)}) \tag{53}$$

for any function $q := (r, u, v)^T$ *satisfying* $\mathbb{P}_{\kappa=1}q = 0$.

Proof of Proposition 4.1. Let us define $\check{q}_{\kappa=1} = q^a_{\kappa=1} - \mathbb{P}_{\kappa=1}\mathbb{P}q^0 := (\check{r}_{\kappa=1}, \check{u}_{\kappa=1})^T$. By multiplying (32)(a) verified by $\check{q}_{\kappa=1}$ with $\check{q}_{\kappa=1}$ itself and by integrating over Ω, we obtain

$$\frac{1}{2}\frac{d}{dt}(\|\check{q}_{\kappa=1}(t)\|^2) = -\frac{a_*\Delta x}{2M}(\|\nabla\check{r}_{\kappa=1}(t)\|^2_{L^2(\Omega)} + \|\partial_x\check{u}_{\kappa=1}(t)\|^2_{L^2(\Omega)} + \|\partial_y\check{v}_{\kappa=1}(t)\|^2_{L^2(\Omega)}). \tag{54}$$

Now, through (52) and (53), we obtain

$$\frac{d}{dt}(\|\check{q}_{\kappa=1}(t)\|^2) + \frac{a_* \Delta x}{M L_\Omega^2}\|\check{q}_{\kappa=1}(t)\|^2 \leqslant 0.$$

We obtain (48) by applying Grönwall's lemma. □

Proof of Corollary 4.1. We have

$$\|q_\kappa^a(t) - \mathbb{P}q^0\| = \|(q_\kappa^a(t) - \mathbb{P}_\kappa \mathbb{P}q^0) - (\mathbb{P}q^0 - \mathbb{P}_\kappa \mathbb{P}q^0)\| \geqslant \|\|q_\kappa^a(t) - \mathbb{P}_\kappa \mathbb{P}q^0\| - \|(\mathbf{1} - \mathbb{P}_\kappa)\mathbb{P}q^0\|\|,$$

by using the reverse triangle inequality. But, inequality (48) shows that

$$\|(1 - \mathbb{P}_{\kappa=1})\mathbb{P}q^0\| \geqslant \|q_{\kappa=1}^a(t) - \mathbb{P}_{\kappa=1}\mathbb{P}q^0\|.$$

Thus, we have also

$$\|q_{\kappa=1}^a(t) - \mathbb{P}q^0\| \geqslant \|(\mathbf{1} - \mathbb{P}_{\kappa=1})\mathbb{P}q^0\| - \|q_{\kappa=1}^a(t) - \mathbb{P}_{\kappa=1}\mathbb{P}q^0\|.$$

We obtain (49) by using again inequality (48). We deduce (50) from (49) by noting that $1 - \exp(-x/2) \geqslant x/3$ for x sufficiently small. In the same way, we deduce (51) from (49) by noting that $1 - \exp(-x/2) \geqslant 1 - \exp(-1/2)$ for any $x \geqslant 1$. □

Proof of Lemma 4.4. This is easily proven by integration of the first component of (32)(a) over Ω, by integration of the second component of (32)(a) over $[a_1, b_1]$ and by integration of the third component of (32)(a) over $[a_2, b_2]$, invoking the periodicity of the domain and the fact that (52) is true at $t = 0$ by definition. □

Proof of Lemma 4.5. This is easily proven by standard Poincaré–Wirtinger inequalities. □

5. Analysis of Godunov type schemes

When the mesh is triangular or tetrahedral, we cannot apply directly the analysis proposed in Section 4 since it is difficult to generalize the notion of modified equation when the mesh is not cartesian. *Nevertheless, the notion of kernel remains relevant in the discrete case for any mesh type*. Thus, to obtain information at the discrete level without the notion of modified equation, the first point is to define the discrete stationary subspace $Ker\mathbb{L}_{\kappa,h}$ that is the discrete version of the stationary subspace *Ker L* (we recall that $\mathcal{E} = KerL$), $\mathbb{L}_{\kappa,h}$ being the discrete version of L_κ given by (33) ($\mathbb{L}_{\kappa,h}$ will be defined below). We will see that when the mesh is triangular, $Ker\mathbb{L}_{\kappa,h}$ is a good approximation of $\mathcal{E}$ when the scheme is the Godunov scheme ($\kappa = 1$) or the *low Mach Godunov scheme* ($\kappa = 0$). This result justifies the fact that Godunov type schemes are accurate at low Mach number when the mesh is triangular. Let us note that the results obtained in the sequel in dimension two on a triangular mesh are also valid in dimension three in the case of a tetrahedral mesh. For the sake of completeness, we will also show that when the mesh is cartesian, $Ker\mathbb{L}_{\kappa,h}$ is a good approximation of $\mathcal{E}$ only in the case of the *low Mach Godunov scheme*.

5.1. Link between the accuracy of Godunov type schemes and the structure of $Ker\mathbb{L}_{\kappa,h}$

The semi-discrete version of Godunov scheme (16) and of *low Mach Godunov scheme* (17) applied to the linear wave equation are given by

$$\frac{dq_h}{dt} + \frac{\mathbb{L}_{\kappa,h}}{M} q_h = 0, \tag{55}$$

with an initial condition $q_h(t = 0)$ which will be defined later (see (64) below). In (55), we have set $q_h := \begin{pmatrix} r \\ \mathbf{u} \end{pmatrix} \in \mathbb{R}^{3N}$ and

$$\begin{cases} \mathbb{L}_{\kappa,h} := \begin{pmatrix} \mathbb{L}_{\kappa,h}^1 \\ \vdots \\ \mathbb{L}_{\kappa,h}^i \\ \vdots \\ \mathbb{L}_{\kappa,h}^N \end{pmatrix}, \\ \mathbb{L}_{\kappa,h}^i q := \frac{a_*}{2|T_i|} \begin{pmatrix} \sum_{A_{ij} \subset \partial T_i} |A_{ij}| \left[(r_i - r_j) + (\mathbf{u}_i + \mathbf{u}_j) \cdot \mathbf{n}_{ij} \right] \\ \sum_{A_{ij} \subset \partial T_i} |A_{ij}| \left[(r_i + r_j) + \kappa(\mathbf{u}_i - \mathbf{u}_j) \cdot \mathbf{n}_{ij} \right] \mathbf{n}_{ij} \end{pmatrix} \end{cases} \tag{56}$$

(N is the number of cells of the mesh). Godunov scheme (16) is defined with (55), (56) and $\kappa = 1$; *low Mach Godunov scheme* (17) is defined with (55), (56) and $\kappa = 0$. The set $Ker\mathbb{L}_{\kappa,h}$ is defined as the set of $\left\{ q := \begin{pmatrix} r \\ \mathbf{u} \end{pmatrix} \in \mathbb{R}^{3N} \right\}$ such that

$$\forall i \in \{1,\dots,N\} : \begin{cases} \sum_{A_{ij}\subset\partial T_i} |A_{ij}| \left[(r_i - r_j) + (\mathbf{u}_i + \mathbf{u}_j)\cdot \mathbf{n}_{ij} \right] = 0, & \text{(a)} \\ \sum_{A_{ij}\subset\partial T_i} |A_{ij}| \left[(r_i + r_j) + \kappa(\mathbf{u}_i - \mathbf{u}_j)\cdot \mathbf{n}_{ij} \right] \mathbf{n}_{ij} = 0. & \text{(b)} \end{cases} \tag{57}$$

Of course, $Ker\mathbb{L}_{\kappa,h}$ is a subspace and we can define its orthogonal $(Ker\mathbb{L}_{\kappa,h})^{\perp}$. Since $\mathbb{R}^{3N}$ is a finite dimension space, we have $Ker\mathbb{L}_{\kappa,h} \oplus (Ker\mathbb{L}_{\kappa,h})^{\perp} = \mathbb{R}^{3N}$ and we can define the discrete orthogonal projection $\mathbb{P}_{\kappa,h}$ on $Ker\mathbb{L}_{\kappa,h}$. The subspace $Ker\mathbb{L}_{\kappa,h}$ is of course invariant since it is stationary by construction. By admitting that the energy $E(t) := \|q(t)\|^2$ (with $\|q\|^2 = \sum_i (r_i^2 + |\mathbf{u}_i|^2)|T_i|$) is a decreasing function for scheme (55), we deduce from the invariance of $Ker\mathbb{L}_{\kappa,h}$ that

$$\|q^0 - \mathbb{P}_{\kappa,h} q^0\| = \mathcal{O}(M) \Rightarrow \|q_h - \mathbb{P}_{\kappa,h} q_h\|(t \geqslant 0) = \mathcal{O}(M). \tag{58}$$

We may think that estimate (58) – that seems to be similar to (34) – implies that Godunov type schemes are accurate at low Mach number on any mesh. But, we know that this is not the case, at least when the mesh is a 2D or 3D cartesian mesh as it was underlined with estimate (36). *The important point here is that $Ker\mathbb{L}_{\kappa,h}$ is not always a good approximation of the well-prepared subspace $\mathcal{E}$.* As a consequence, $\mathbb{P}_{\kappa,h}$ is not always a good approximation of the Hodge projection $\mathbb{P}$. *In that case, estimate (58) cannot be considered as a discrete version of estimate (34).* More precisely, we will prove in the sequel that $Ker\mathbb{L}_{\kappa,h}$ is a good approximation of $\mathcal{E}$ when the mesh is a triangular mesh for $\kappa \in \{0, 1\}$. Moreover, we will also prove that $Ker\mathbb{L}_{\kappa,h}$ is a good approximation of $\mathcal{E}$ when the mesh is rectangular if and only if $\kappa = 0$. At last, let us emphasize that $Ker\mathbb{L}_{\kappa=1,h} \neq Ker\mathbb{L}_{\kappa=0,h}$ since for the Godunov scheme ($\kappa = 1$) and for the *low Mach Godunov scheme* ($\kappa = 0$), Eq. (57)(b) is respectively defined by

$$\forall i \in \{1,\dots,N\} : \sum_{A_{ij}\subset\partial T_i} |A_{ij}| \left[(r_i + r_j) + (\mathbf{u}_i - \mathbf{u}_j)\cdot \mathbf{n}_{ij} \right] \mathbf{n}_{ij} = 0, \tag{59}$$

and

$$\forall i \in \{1,\dots,N\} : \sum_{A_{ij}\subset\partial T_i} |A_{ij}| (r_i + r_j) \mathbf{n}_{ij} = 0. \tag{60}$$

More precisely, we will prove that

$$\begin{cases} \text{on a triangular or tetrahedral mesh :} & Ker\mathbb{L}_{\kappa=1,h} = \mathcal{E}_h^{\Delta} \subset Ker\mathbb{L}_{\kappa=0,h}, \\ \text{on a 1D cartesian mesh :} & Ker\mathbb{L}_{\kappa=1,h} = \mathcal{E}_h^{\square} = Ker\mathbb{L}_{\kappa=0,h}, \\ \text{on a 2D or 3D cartesian mesh :} & Ker\mathbb{L}_{\kappa=1,h} \supsetneq \mathcal{E}_h^{\square} = Ker\mathbb{L}_{\kappa=0,h}, \end{cases}$$

where $\mathcal{E}_h^{\Delta}$ and $\mathcal{E}_h^{\square}$ – respectively defined by (20) and (23) – are standard discretizations of the continuous well-prepared subspace $\mathcal{E}$ when the mesh is respectively triangular and cartesian.

In the sequel, we define for the discrete solution $q_h(t)$ of semi-discrete scheme (55) the splitting

$$q_h(t) = q^a_{\kappa,h}(t) + q^b_{\kappa,h}(t). \tag{61}$$

In (61), $q^a_{\kappa,h}(t)$ is solution of (55) with the initial condition

$$q^a_{\kappa,h}(t=0) = \mathbb{P}_h(\mathbb{P}q^0)_h, \tag{62}$$

and $q^b_{\kappa,h}(t)$ is solution of (55) with the initial condition

$$q^b_{\kappa,h}(t=0) = q^0_h - (\mathbb{P}q^0)_h, \tag{63}$$

where $\mathbb{P}_h := \mathbb{P}_{\mathcal{E}_h^{\Delta}}$, $\mathbb{P}_h := \mathbb{P}_{\mathcal{E}_h^{\square}}$ or $\mathbb{P}_h := \mathbb{P}_{\mathcal{E}_h^{MAC,\square}}$ according to mesh type, and where $(q^0)_h$ and $(\mathbb{P}q^0)_h$ are accurate approximations of respectively q^0 and $\mathbb{P}q^0$. Relations (61)–(63) are discrete versions of (41)–(43). In the sequel, we suppose that the initial condition q^0 is well-prepared, which implies that $\|q^b_{\kappa,h}(t=0)\| = \mathcal{O}(M)$. Let us underline that (62) and (63) imply that the initial condition $q_h(t=0)$ of (55) is given by

$$q_h(t=0) = \mathbb{P}_h(\mathbb{P}q^0)_h + q^0_h - (\mathbb{P}q^0)_h. \tag{64}$$

We have defined this initial condition instead of q^0_h to be sure that it is a sum of an element of the discrete well-prepared subspace and of an element of order $\mathcal{O}(M)$. And, by stability of the Godunov scheme and of the *low Mach Godunov scheme*, we have $\|q^b_{\kappa,h}(t \geqslant 0)\| = \mathcal{O}(M)$. This means that the accuracy of these schemes will be completely determined by the behaviour of $q^a_{\kappa,h}(t)$ which deeply depends on the structure of $Ker\mathbb{L}_{\kappa,h}$.

5.2. The case of triangular meshes

We now study the discrete version of the results proposed in Section 4.2 when the mesh is a 2D triangular mesh, the 3D tetrahedral case being similar.

5.2.1. Structure of $Ker\mathbb{L}_{\kappa,h}$ when the mesh is triangular

The following result holds (the proof is in annex A):

Lemma 5.1. *When the mesh is triangular, we have*

$$Ker\mathbb{L}_{\kappa=1,h} = \mathcal{E}_h^{\Delta}, \tag{65}$$

and

$$Ker\mathbb{L}_{\kappa=0,h} \supset \mathcal{E}_h^{\Delta}. \tag{66}$$

Moreover, any $q := (r, \mathbf{u})^T \in Ker\mathbb{L}_{\kappa=0,h}$ is such that $\exists c \in \mathbb{R}$ such that $\forall T_i : \ r_i = c$.

Equality (65) means that $Ker\mathbb{L}_{\kappa=1,h}$ is a good approximation of $\mathcal{E}$. The strict inclusion (66) implies that $Ker\mathbb{L}_{\kappa=0,h}$ is rich enough to well approach $\mathcal{E}$: in that sense, we can also say that $Ker\mathbb{L}_{\kappa=0,h}$ is a good approximation of $\mathcal{E}$. At last, let us underline that the fact that the elements T_i are all triangles is essential in the proof of Lemma 5.1; a similar result would not be obtained for other types of elements as we will see in Section 5.3.

5.2.2. Time behaviour when the mesh is triangular

As discussed at the end of Section 5.1, we have $\|q^b_{\kappa\in\{0,1\},h}(t \geqslant 0)\| = \mathcal{O}(M)$. Moreover, by construction, we have $q^a_{\kappa\in\{0,1\},h}(t \geqslant 0) = q^a_{\kappa\in\{0,1\},h}(t = 0) \in \mathcal{E}_h^{\Delta}$. In that case, there are no spurious acoustic waves and, thus, there is no condition on h to avoid the creation of spurious acoustic waves for the Godunov scheme and for the *low Mach Godunov scheme*. This theoretical result justifies the numerical results proposed in Section 3.5.

5.3. The case of cartesian meshes

We now study the discrete version of the results proposed in Section 4.2 when the mesh is a 2D cartesian mesh, the 3D cartesian case being similar. For the sake of simplicity, we suppose, as in Section 3.4.2, that the number of cells N_x and N_y in each direction are odd. This hypothesis allows us to forget the possible existence of checkerboard modes due to the even/odd decoupling. Nevertheless, it would be possible to extend the following results when N_x and/or N_y are even.

5.3.1. Structure of $Ker\mathbb{L}_{\kappa,h}$ when the mesh is cartesian

We have the following result (the proof is in annex A):

Lemma 5.2. *When $\Omega = \mathbb{T}^{d=2}$ and when the mesh is cartesian, we have*

$$Ker\mathbb{L}_{\kappa=1,h} = \left\{ q := \begin{pmatrix} r \\ \mathbf{u} \end{pmatrix} \in \mathbb{R}^{3N_xN_y} \quad \text{such that } \exists (c,(u_j),(v_i)) \in \mathbb{R}\times\mathbb{R}^{N_y}\times\mathbb{R}^{N_x} \quad \text{such that } \forall (i,j) : r_{i,j} = c \quad \text{and } \mathbf{u}_{i,j} = \begin{pmatrix} u_j \\ v_i \end{pmatrix} \right\}, \tag{67}$$

which implies that

$$Ker\mathbb{L}_{\kappa=1,h} \subsetneq \mathcal{E}_h^{\square}. \tag{68}$$

Moreover, we have

$$Ker\mathbb{L}_{\kappa=0,h} = \mathcal{E}_h^{\square}. \tag{69}$$

Relations (67) and (68) show that the subspace $Ker\mathbb{L}_{\kappa=1,h}$ is a very poor subspace of $\mathcal{E}$. Indeed, the subspace defined with (67) is unable to approach all divergence-free continuous functions. On the other hand, (69) show that $Ker\mathbb{L}_{\kappa=0,h}$ is rich enough to approach all divergence-free continuous functions. In other words, $Ker\mathbb{L}_{\kappa=0,h}$ is a good approximation of $\mathcal{E}$. These results are coherent with those obtained in Section 4.2, Lemma 5.2 being the discrete version of Lemma 4.2.

Let us note that when N_x or N_y are even, we only have $Ker\mathbb{L}_{\kappa=0,h} \supset \mathcal{E}_h^{\square}$. This difference between $Ker\mathbb{L}_{\kappa=0,h}$ and $\mathcal{E}_h^{\square}$ is linked to the existence of checkerboard modes. Of course, since they belong to the kernel of the *low Mach number Godunov scheme*, they do not grow up with time (see [23] for a study of these checkerboard modes in the 1D case).

5.3.2. Time behaviour when the mesh is cartesian

We now study the time behaviour of the solution $q_h(t)$ of semi-discrete scheme (55) when the mesh is cartesian.

- **The case of the Godunov scheme ($\kappa = 1$) on a cartesian mesh**:

For the sake of simplicity, we now suppose that $\Delta x = \Delta y := h$. We reach the same conclusions as in the analysis conducted with the first-order modified equation in Section 4.2.2. More precisely, let us define

$$\hat{q}_h^0 := \mathbb{P}_h(\mathbb{P}q^0)_h.$$

The vector $\hat{q}_h^0$ belongs to $\mathcal{E}_h^{\square}$ (since $\mathbb{P}_h := \mathbb{P}_{\mathcal{E}_h^{\square}}$) and defines the initial condition of $q^a_{\kappa=1,h}(t)$ solution of (55) (see the discussion at the end of Section 5.1). Let us underline that $\hat{q}_h^0$ is close to $(\mathbb{P}q^0)_h$. The fact that $\hat{q}_h^0 - \mathbb{P}_{\kappa=1,h}\hat{q}_h^0$ is in general of order one (because of strict inclusion (68)) leads to the fact that

$$\|q^a_{\kappa=1,h}(t) - \hat{q}_h^0\| \geqslant \mathcal{O}(h) \quad \text{when } t = \mathcal{O}(M). \tag{70}$$

Estimate (70) is a discrete version of estimate (44). As in the case of first-order modified equation (32) studied at the continuous level (see *point 3* in Section 4.2.2), we cannot deduce directly from (70) a discrete version of estimate (36) that would characterizes the creation of discrete spurious acoustic waves in the discrete acoustic subspace $(\mathcal{E}_h^{\square})^{\perp}$. Indeed, any discrete version of (36) would be stronger than (70). Nevertheless, knowing that (36) was proven at the continuous level in [9] in the case of first-order modified equation, we may consider (70) as a direct consequence of the creation of discrete spurious acoustic waves. Let us note that (36) is experimentally justified in Section 3.5. As a consequence, the constraint on the mesh to avoid the creation of spurious acoustic waves of order one within a time of order $\mathcal{O}(M)$ should be

$$h = \mathcal{O}(M) \tag{71}$$

for the Godunov scheme in the cartesian case *which is too restrictive for practical applications*. Moreover, we also obtain that

$$\|q^a_{\kappa=1,h}(t) - \hat{q}_h^0\| \geqslant \mathcal{O}(1) \quad \text{when } t = \mathcal{O}\left(\frac{M}{\Delta x}\right), \tag{72}$$

which is a direct consequence of the fast diffusion of $\hat{q}_h^0$ toward $\mathbb{P}_{\kappa=1,h}\hat{q}_h^0$ when t grows (see Proposition 5.1 below). Estimate (72) is a discrete version of estimate (47). Figs. 5 and 6 confirm this fast diffusion for the velocity field $\mathbf{u}$ on a 2D cartesian mesh of 51×51 cells in the case of the numerical test-case proposed in Section 3.5. Indeed, Fig. 5 represents isolines of $\psi_{i,j}(t = 20\ M)$ where $\psi_{i,j}$ is deduced from discrete projection (25) of $q_h(t = 20\ M)$ onto $\mathcal{E}_h^{\square}$; and Fig. 6 represents isolines of $\psi_{th}(x,y) := -\frac{1}{4\pi}[\cos(2\pi x) + \cos(4\pi y)]$ which is deduced from the projection of initial condition (30) onto $KerL_{\kappa=1}$ defined by (37). Indeed, from Lemma 4.3, the velocity component of this projection is given by $(\sin(4\pi y), -\frac{1}{2}\sin(2\pi x))^T = \nabla \times \psi_{th}$. On the other hand, Figs. 1 and 2 in Section 3.5 show that the projection of q_h onto $(\mathcal{E}_h^{\square})^{\perp}$ converges toward zero when t grows. Thus, Figs. 1, 2 and 5, 6 show that q_h converge toward $\mathbb{P}_{\kappa=1,h}\hat{q}_h^0$ when$q_h(t = 0) = \hat{q}_h^0$.

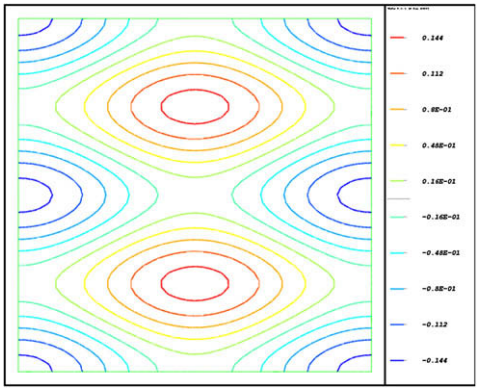

Fig. 5. Isolines of $\psi_{i,j}(t = 20\ \mathrm{M})$. Godunov scheme on a 51×51 cartesian mesh.

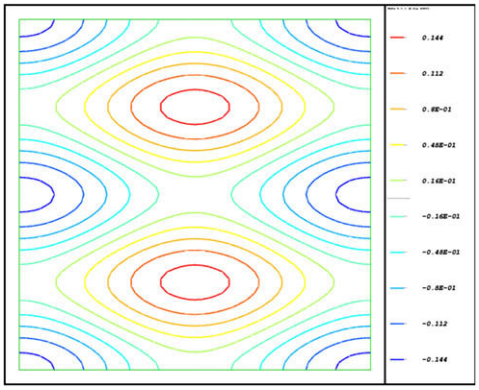

Fig. 6. Isolines of $\psi_{th}(x,y)$. Theoretical result on a 51×51 cartesian mesh.

In order to prove (70) and (72), we use discrete versions of Lemma 4.3, of Proposition 4.1 and of Corollary 4.1. The discrete version of Lemma 4.3 is given by:

Lemma 5.3. *When $\Omega = \mathbb{T}^{d=2}$ and when the mesh is cartesian, the projection $\mathbb{P}_{\kappa=1,h}$ is defined by*

$$(\mathbb{P}_{\kappa=1,h} q_h)_{i,j} = \begin{pmatrix} \dfrac{1}{N_x N_y} \displaystyle\sum_{k,\ell} (r_h)_{k,\ell} \\ \dfrac{1}{N_x} \displaystyle\sum_{k} (u_h)_{k,j} \\ \dfrac{1}{N_y} \displaystyle\sum_{\ell} (v_h)_{i,\ell} \end{pmatrix}.$$

Lemma 5.3 written in 1D ($d = 1$) or in 3D ($d = 3$) is similar. The discrete version of Proposition 4.1 is given by:

Proposition 5.1. *When $\kappa = 1$, there exists a constant L_Ω depending only on Ω such that*

$$\forall t \geqslant 0 : \|q^a_{\kappa=1,h}(t) - \mathbb{P}_{\kappa=1,h} \hat{q}^0_h\| \leqslant \|(\mathbf{1} - \mathbb{P}_{\kappa=1,h}) \hat{q}^0_h\| \exp\left(-\frac{a_* h}{2ML^2_\Omega} t\right). \tag{73}$$

And, from this proposition, we easily obtain a discrete version of Corollary 4.1 that allows to obtain estimates (70) and (72).

- **The case of the** *low Mach Godunov scheme* **($\kappa = 0$) on a cartesian mesh:**

As discussed at the end of Section 5.1, we have $\|q^b_{\kappa,h}(t \geqslant 0)\| = \mathcal{O}(M)$. Moreover, by construction, we have $q^a_{\kappa,h}(t \geqslant 0) = q^a_{\kappa,h}(t = 0) \in \mathcal{E}^{\square}_h$ (we recall that $Ker \mathbb{L}_{\kappa=0,h} = \mathcal{E}^{\square}_h$). In that case, there are no spurious acoustic waves and, thus, there is no condition on h to avoid the creation of spurious acoustic waves. This theoretical result justifies the numerical results proposed in Section 3.5.

The proof of Proposition 5.1 uses discrete versions of Lemmas 4.4 and 4.5. The discrete version of Lemma 4.4 is given by:

Lemma 5.4. *We have*

$$\forall t \geqslant 0 : \mathbb{P}_{\kappa=1,h}(q^a_{\kappa=1,h}(t) - \mathbb{P}_{\kappa=1,h} \hat{q}^0_h) = 0. \tag{74}$$

Before we turn to the next lemma, we need definitions of discrete differential operators. Let $u_h = (u_{i,j})$ be in $\mathbb{R}^{N_x N_y}$, we define $\partial_{x,h} u_h$ by

$$\forall (i,j) \in [0, N_x] \times [1, N_y] : (\partial_{x,h} u_h)_{i+1/2,j} := \frac{u_{i+1,j} - u_{i,j}}{\Delta x}. \tag{75}$$

Let $v_h = (v_{i,j})$ be in $\mathbb{R}^{N_x N_y}$, we define $\partial_{y,h} v_h$ by

$$\forall (i,j) \in [1, N_x] \times [0, N_y] : (\partial_{y,h} v_h)_{i,j+1/2} := \frac{v_{i,j+1} - v_{i,j}}{\Delta y}. \tag{76}$$

Let $r_h = (r_{i,j})$ be in $\mathbb{R}^{N_x N_y}$. We define $\nabla_h r_h$ by

$$\begin{cases} \forall (i,j) \in [0, N_x] \times [1, N_y] : (\nabla_h r_h)_{i+1/2,j} := (\partial_{x,h} r_h)_{i+1/2,j}, & \text{(a)} \\ \forall (i,j) \in [1, N_x] \times [0, N_y] : (\nabla_h r_h)_{i,j+1/2} := (\partial_{y,h} r_h)_{i,j+1/2}. & \text{(b)} \end{cases} \tag{77}$$

In (75), it is meant, by periodicity of the domain, that $u_{0,j} = u_{N_x,j}$ and $u_{N_x+1,j} = u_{1,j}$. The same kind of convention is used in (77)(a). In the same way, it is meant in (76) that $v_{i,0} = v_{i,N_y}$ and $v_{i,N_y+1} = v_{i,1}$, and the same convention is used in (77)(b). The discrete version of Lemma 4.5 is given by:

Lemma 5.5. *There exists a constant L_Ω depending only on Ω such that*

$$\forall t \geqslant 0 : \|q_h(t)\|^2 \leqslant L^2_\Omega \left(\|\nabla_h r_h(t)\|^2_{L^2(\Omega)} + \|\partial_{x,h} u_h(t)\|^2_{L^2(\Omega)} + \|\partial_{y,h} v_h(t)\|^2_{L^2(\Omega)} \right) \tag{78}$$

for any function q_h satisfying $\mathbb{P}_{\kappa=1,h} q_h = 0$.

Proof of Proposition 5.1. Let us define $\check{q}_{\kappa=1,h} = q^a_{\kappa=1,h} - \mathbb{P}_{\kappa=1} \hat{q}^0_h := (\check{r}_{\kappa=1,h}, \check{u}_{\kappa=1,h})^T$. By multiplying (55) verified by $\check{q}_{\kappa=1,h}$ with $\check{q}_{\kappa=1,h}$ itself and by performing discrete integrations, we obtain

$$\frac{1}{2} \frac{d}{dt} (\|\check{q}_{\kappa=1,h}(t)\|^2) = -\frac{a_* h}{2M} \left(\|\nabla_h \check{r}_{\kappa=1,h}(t)\|^2_{L^2(\Omega)} + \|\partial_{x,h} \check{u}_{\kappa=1,h}(t)\|^2_{L^2(\Omega)} + \|\partial_{y,h} \check{v}_{\kappa=1,h}(t)\|^2_{L^2(\Omega)} \right).$$

Now, through (74) and (78), we obtain

$$\frac{d}{dt}(\|\check{q}_{\kappa=1,h}(t)\|^2)+\frac{a_* h}{ML_\Omega^2}\|\check{q}_{\kappa=1,h}(t)\|^2\leqslant 0.$$

We conclude, like in the proof of Proposition 4.1, by using Grönwall's lemma. □

Proof of Lemma 5.4. This is easily proven by summation of the first component of (55) over $(k,\ell)\in[1,N_x]\times[1,N_y]$, by summation of the second component of (55) over $k\in[1,N_x]$ and by summation of the third component of (55) over $\ell\in[1,N_y]$, invoking the periodicity of the domain, the conservativity of the scheme and the fact that (74) is true at $t=0$ by definition. □

Proof of Lemma 5.5. We obtain the result by using a discrete Poincaré–Wirtinger inequality [24]. □

5.4. The monodimensional case

In the 1D case, the discrete well-prepared subspace $\mathcal{E}_h^{\square}$ (given in 2D by (23)) is defined by

$$\mathcal{E}_h^{\square}=\left\{q:=\begin{pmatrix}r\\u\end{pmatrix}\in\mathbb{R}^{2N_x}\quad\text{such that }\exists(a,b)\in\mathbb{R}^2\quad\text{such that }\forall i:\ r_i=a\quad\text{and }u_i=b\right\}$$

(N_x is the number of cells supposed to be odd for the sake of simplicity) and Lemma 5.2 is replaced by:

Lemma 5.6. *When $\Omega=\mathbb{T}^{d=1}$, we have*

$$Ker\mathbb{L}_{\kappa=1}=\mathcal{E}_h^{\square}. \tag{79}$$

Moreover, we have

$$Ker\mathbb{L}_{\kappa=0,h}=\mathcal{E}_h^{\square}. \tag{80}$$

Here, the important point is that (79) is completely different from (68) (nevertheless, (80) is identical to (69)). Thus, this lemma underlines that the Godunov scheme (and the *low Mach Godunov scheme* as we already known) do not suffer of any inaccuracy at low Mach number, which is coherent with estimate (34) obtained in [9] by studying at the continuous level first-order modified equation (32).

6. Analysis of the MAC scheme

We now show that the point of view proposed in Section 5 is compatible with the fact that a MAC type scheme [26] is adapted to solve the compressible Euler or Navier–Stokes system at low Mach number. We recall that the MAC scheme applied to linear wave equation (1) is given by (18). In that case, the discrete linear operator $\mathbb{L}_h$ is defined by

$$\left\{\mathbb{L}_h:=\begin{pmatrix}\mathbb{L}_h^{1,1}\\ \vdots\\ \mathbb{L}_h^{i,j}\\ \vdots\\ \mathbb{L}_h^{N_x,N_y}\end{pmatrix},\quad \mathbb{L}_h^{i,j}q:=a_*\begin{pmatrix}\dfrac{u_{i+1/2,j}-u_{i-1/2,j}}{\Delta x}+\dfrac{v_{i,j+1/2}-v_{i,j-1/2}}{\Delta y}\\ \dfrac{r_{i+1,j}-r_{i,j}}{\Delta x}\\ \dfrac{r_{i,j+1}-r_{i,j}}{\Delta y}\end{pmatrix}\right. . \tag{81}$$

We can prove that the kernel of $\mathbb{L}_h$ is now given by

$$Ker\mathbb{L}_h=\mathcal{E}_h^{MAC,\square}, \tag{82}$$

where $\mathcal{E}_h^{MAC,\square}$ is defined by (27). Thus, the behaviour of the MAC scheme on a cartesian mesh is identical to the one of the Godunov scheme ($\kappa=1$) on a triangular mesh (see (65)) or to the one of the *low Mach Godunov scheme* ($\kappa=0$) on a triangular mesh (see (66)) or on a cartesian mesh (see (69)). In that case, there are no spurious acoustic waves and, thus, there is no condition on h to avoid the creation of spurious acoustic waves. This theoretical result justifies the numerical results proposed in Section 3.5. Let us underline that there are no checkerboard modes in the case of the MAC scheme, which is not the case for the *low Mach Godunov scheme* when N_x or N_y are even (see [23] in the 1D case).

7. Link with the asymptotic analysis

The analysis of discretized compressible Euler system at low Mach number is often performed through a formal asymptotic analysis in powers of M [10,13,21,22]. In the case of numerical scheme (55), if we set

$$q_i^n = q_i^{0,n} + Mq_i^{1,n} + \cdots, \tag{83}$$

then, the development of (55) in powers of M formally yields that the set $(q_i^{0,n})$ belongs to $Ker\mathbb{L}_{\kappa,h}$ at each time t^n, while, in the continuous linear wave equation (1), the $\mathcal{O}(1)$ term of the development belongs to $\mathcal{E}$. But, we have shown in Section 5 that

$$\begin{cases} \text{on a triangular or tetrahedral mesh :} & Ker\mathbb{L}_{\kappa=1,h} = \mathcal{E}_h^{\Delta} \subset Ker\mathbb{L}_{\kappa=0,h}, \quad \text{(a)} \\ \text{on a 1D cartesian mesh :} & Ker\mathbb{L}_{\kappa=1,h} = \mathcal{E}_h^{\square} = Ker\mathbb{L}_{\kappa=0,h}, \quad \text{(b)} \\ \text{on a 2D or 3D cartesian mesh :} & Ker\mathbb{L}_{\kappa=1,h} \subsetneq \mathcal{E}_h^{\square} = Ker\mathbb{L}_{\kappa=0,h}, \quad \text{(c)} \end{cases} \tag{84}$$

where $\mathcal{E}_h^{\Delta}$ and $\mathcal{E}_h^{\square}$ – respectively defined by (20) and (23) – are standard discretizations of the continuous well-prepared subspace $\mathcal{E}$ when the mesh is respectively triangular and cartesian. Then, $(q_i^{0,n}) \in Ker\mathbb{L}_{\kappa,h}$ implies that

$$\forall i : r_i^{0,n} = c \quad \text{that is to say } \forall i : r_i^n = c + \mathcal{O}(M) \tag{85}$$

for any mesh type ((85) is a direct consequence of (89); see annex A). Nevertheless, (85) is not sufficient to prove that numerical scheme (55) is or is not accurate at low Mach number. Indeed, a necessary condition for the numerical asymptotic development of q to be a good approximation of the continuous one is that $Ker\mathbb{L}_{\kappa,h}$ approaches $\mathcal{E}$ well enough, which is only verified when the mesh is triangular (or tetrahedral) or 1D cartesian in the case of the Godunov scheme ($\kappa = 1$) and when the mesh is triangular (or tetrahedral) as well as cartesian in the case of the *low Mach Godunov scheme* ($\kappa = 0$) because of (84). Let us underline that these remarks concern also MAC scheme (18) whose behaviour is identical to the one of the *low Mach Godunov scheme* on a cartesian mesh (compare (82) and (84)(c) with $\kappa = 0$).

8. Conclusion

In this article, we have studied the behaviour of the Godunov scheme, of the *low Mach Godunov scheme* [9] and of the MAC scheme applied to the linear wave equation in order to study the behaviour of these schemes applied to the resolution of the compressible Euler or Navier–Stokes system at low Mach number over short (*i.e.* acoustic) time scales. We have enlightened the influence of the cell geometry on the accuracy of these schemes. In the triangular or tetrahedral case and in the 1D cartesian case, the stationary space of the Godunov scheme approaches well enough the continuous space of constant pressure and divergence-free velocity, while this is not the case in the 2D or 3D cartesian case. In the triangular or tetrahedral case and in the 1D, 2D or 3D cartesian case, the stationary space of the *low Mach Godunov scheme* approaches well enough the continuous space of constant pressure and divergence-free velocity. In the 1D, 2D or 3D cartesian case, the stationary space of the MAC scheme approaches well enough the continuous space of constant pressure and divergence-free velocity. As a consequence, it is easy to construct a discrete constant pressure and divergence-free velocity initial condition in such a way there is no discrete spurious acoustic waves for the Godunov scheme and for the *low Mach Godunov scheme* in the triangular or tetrahedral case, this remark being also valid for the *low Mach Godunov scheme* and for the MAC scheme in the 1D, 2D or 3D cartesian case and for the Godunov scheme only in the 1D cartesian case. As a consequence, for flows in the low Mach regime, the fast diffusion of the initial condition to its projection in the stationary space of the scheme has a dramatic effect on the accuracy of the Godunov scheme in the 2D or 3D cartesian case (but not in the 1D cartesian case), since it creates a spurious acoustic wave of order Δx within a time of order M. On the contrary, at low Mach number, the Godunov scheme and the *low Mach Godunov scheme* remain accurate in the triangular or tetrahedral case, the Godunov scheme remains accurate in the 1D cartesian case, the *low Mach Godunov scheme* and the MAC scheme remain accurate in the 1D, 2D or 3D cartesian case. Note that these conclusions are only valid when the boundary conditions are periodic: non-periodic boundary conditions may require additional analysis that was not performed in the present work.

Appendix A. Proof of Lemmas 5.1 and 5.2

We first start with calculations that are common to both lemmas. Let us consider $q_h := (r_i, \mathbf{u}_i)^T \in Ker\mathbb{L}_{\kappa,h}$, *i.e.* verifying (57). Let us multiply (57)(a) by r_i and (57)(b) by $\mathbf{u}_i$ and add the resulting equalities over i. Then, we have

$$\begin{cases} \displaystyle\sum_i \sum_{A_{ij} \subset \partial T_i} |A_{ij}|[r_i(r_i - r_j) + r_i(\mathbf{u}_i + \mathbf{u}_j) \cdot \mathbf{n}_{ij}] = 0, & \text{(a)} \\ \displaystyle\sum_i \sum_{A_{ij} \subset \partial T_i} |A_{ij}|[(r_i + r_j) + \kappa(\mathbf{u}_i - \mathbf{u}_j) \cdot \mathbf{n}_{ij}](\mathbf{u}_i \cdot \mathbf{n}_{ij}) = 0. & \text{(b)} \end{cases} \tag{86}$$

Since for all i we have $\sum_{A_{ij}\subset\partial T_i}|A_{ij}|\mathbf{n}_{ij}=0$ (which is valid for any type of mesh), we also have

$$\forall i\in\{1,\dots,N\}:\sum_{A_{ij}\subset\partial T_i}|A_{ij}|r_i\mathbf{u}_i\cdot\mathbf{n}_{ij}=r_i\mathbf{u}_i\cdot\left(\sum_{A_{ij}\subset\partial T_i}|A_{ij}|\mathbf{n}_{ij}\right)=0.$$

By injecting this relation into (86), we obtain

$$\begin{cases}\displaystyle\sum_i\sum_{A_{ij}\subset\partial T_i}|A_{ij}|[r_i(r_i-r_j)+r_i\mathbf{u}_j\cdot\mathbf{n}_{ij}]=0, & \text{(a)}\\ \displaystyle\sum_i\sum_{A_{ij}\subset\partial T_i}|A_{ij}|[r_j+\kappa(\mathbf{u}_i-\mathbf{u}_j)\cdot\mathbf{n}_{ij}](\mathbf{u}_i\cdot\mathbf{n}_{ij})=0. & \text{(b)}\end{cases}\tag{87}$$

Now, we rewrite the sums (87)(a) and (b) as sums over the edges A_{ij}. In these two sums, each individual A_{ij} contributes twice: once when the considered triangle is T_i, and once when it is T_j, for which we have to exchange the roles of i and j in the corresponding contribution. This results in the fact that (87) is equivalent to

$$\begin{cases}\displaystyle\sum_{A_{ij}}|A_{ij}|\{[r_i(r_i-r_j)+r_j(r_j-r_i)]+r_i\mathbf{u}_j\cdot\mathbf{n}_{ij}+r_j\mathbf{u}_i\cdot\mathbf{n}_{ji}\}=0,\\ \displaystyle\sum_{A_{ij}}|A_{ij}|\{r_j\mathbf{u}_i\cdot\mathbf{n}_{ij}+r_i\mathbf{u}_j\cdot\mathbf{n}_{ji}+\kappa(\mathbf{u}_i-\mathbf{u}_j)\cdot\mathbf{n}_{ij}(\mathbf{u}_i\cdot\mathbf{n}_{ij})+\kappa(\mathbf{u}_j-\mathbf{u}_i)\cdot\mathbf{n}_{ji}(\mathbf{u}_j\cdot\mathbf{n}_{ji})\}=0.\end{cases}$$

Adding these two equalities and noting that $\mathbf{n}_{ji}=-\mathbf{n}_{ij}$, we finally obtain

$$\sum_{A_{ij}}|A_{ij}|\{(r_i-r_j)^2+\kappa[(\mathbf{u}_i-\mathbf{u}_j)\cdot\mathbf{n}_{ij}]^2\}=0.\tag{88}$$

This leads to the fact that there exists a constant $c\in\mathbb{R}$ such that

$$\forall i: r_i=c\quad\text{for any }\kappa\in\{0,1\}\tag{89}$$

which means that r is a constant over the whole domain. Let us underline that (88) – and, thus, (89) – is verified *for any mesh type*. Let us now suppose that $\kappa=1$. We also deduce from (88) that we have

$$\forall i:(\mathbf{u}_i-\mathbf{u}_j)\cdot\mathbf{n}_{ij}=0\quad\text{when }\kappa=1\tag{90}$$

for all couples (i,j) such that T_i and T_j are neighboring cells: thus, the normal component of $\mathbf{u}$ is conserved through the edges $\partial T_i\cap\partial T_j$ when $\kappa=1$. As for (89), let us underline that (90) is verified *for any mesh type*.

Proof of Lemma 5.1. We now specialize to the triangular case. We use the following lemma whose proof is in annex Appendix B.

Lemma A.1. *Let us suppose that the mesh is triangular. Then the fact that*

$$\exists(\mathbf{u}_i)\quad\textit{such that }\mathbf{u}_i\cdot\mathbf{n}_{ij}=-\mathbf{u}_j\cdot\mathbf{n}_{ji}\quad\textit{for all neighboring }T_i\quad\textit{and }T_j\tag{91}$$

is equivalent to the fact that

$$\exists(u_{ij})\quad\textit{such that}\begin{cases}\displaystyle\sum_{A_{ij}\subset\partial T_i}|A_{ij}|u_{ij}=0\quad\textit{for all }T_i, & \text{(a)}\\ u_{ij}=-u_{ji}\quad\textit{for all neighboring }T_i\quad\textit{and }T_j. & \text{(b)}\end{cases}\tag{92}$$

Moreover, we have

$$u_{ij}=\mathbf{u}_i\cdot\mathbf{n}_{ij}.$$

The important point is that (92) is equivalent to write that either there exists a constant vector $(a,b)^T$ such that $\mathbf{u}_i=(a,b)^T$ for all $i\in\{1,\dots,N\}$ and $u_{ij}=\mathbf{u}_i\cdot\mathbf{n}_{ij}$, either there exists a set of real-valued (ψ_k) defined at the vertices S_k of the triangles such that if S_{k1} and S_{k2} are two consecutive vertices of T_i (with respect to the positive orientation) and if $_{ij}$ is the subscript of the edge whose vertices are S_{k1} and S_{k2}, then

$$u_{ij}=\frac{\psi_{k2}-\psi_{k1}}{|A_{ij}|}.\tag{93}$$

The fact that a set u_{ij} defined by (93) verifies (92) is obvious; the fact that this is the only possible representation, besides constant vectors $(a,b)^T$, may be inferred, for example, from the adaptation to the periodic case of the works of Nicolaides on covolume schemes [7]. Now, the set of values (ψ_k) associated to the vertices S_k defines a function ψ_h in V_h defined by

(19). It can be checked that the exterior normal component of the curl of this function on the edge A_{ij} is exactly the expression in the right hand side of (93), which itself proves that $\mathbf{u}_i = (\nabla \times \psi_h)_{|T_i}$. Finally, by using (89) and Lemma A.1, we obtain that any $q_h := (r_i, \mathbf{u}_i)^T \in Ker\mathbb{L}_{\kappa=1,h}$ is such that

$$\forall i : r_i = c \quad \text{and } \mathbf{u}_i = (a,b)^T + (\nabla \times \psi_h)_{|T_i},$$

which exactly means that $Ker\mathbb{L}_{\kappa=1,h}$ is equal to $\mathcal{E}_h^A$ defined by (20). On the other side, any function of $\mathcal{E}_h^A$ satisfies also (88) with $\kappa = 0$ – and, thus, satisfies (89) – but does not necessarily satisfy (91). This proves that $Ker\mathbb{L}_{\kappa=0,h} \supset \mathcal{E}_h^A$. □

Proof of Lemma 5.2. We now specialize to the cartesian rectangular case. Let us consider $q := (r, \mathbf{u})^T \in Ker\mathbb{L}_{\kappa,h}$. When $\kappa = 1$, the conservation of the normal component of $\mathbf{u}$ through the common vertical edge of the cells (i,j) and $(i+1,j)$ yields that $u_{ij} = u_{i+1,j}$. Since this is true for all (i,j), we have that for all $j \in [1, N_y]$, there exists a constant u_j such that

$$\forall i \in [1, N_x] : u_{ij} = u_j.$$

In the same way, the conservation of the normal component of $\mathbf{u}$ through the common horizontal edge of the cells (i,j) and $(i,j+1)$ yields that $v_{ij} = v_{ij+1}$. Since this is true for all (i,j), we have that for all $i \in [1, N_x]$, there exists a constant v_i such that

$$\forall j \in [1, N_y] : v_{ij} = v_i.$$

Knowing that (89) is verified, this proves that $Ker\mathbb{L}_{\kappa=1,h}$ is given by (67). Let us now choose $\kappa = 0$. By using again (89), we obtain that (57)(a) is equivalent to

$$\Delta y\big[(u_{i+1,j} + u_{ij}) - (u_{ij} + u_{i-1,j})\big] + \Delta x\big[(v_{ij+1} + v_{ij}) - (v_{ij} + v_{ij-1})\big] = 0,$$

which may be reformulated as

$$\forall (i,j) \in [1, N_x] \times [1, N_y] : \frac{1}{2\Delta x}(u_{i+1,j} - u_{i-1,j}) + \frac{1}{2\Delta y}(v_{ij+1} - v_{ij-1}) = 0. \tag{94}$$

Conversely, each set (r_{ij}, u_{ij}, v_{ij}) satisfying $r_{ij} = c$ and (94) verifies (57) when $\kappa = 0$, that is to say belongs to $Ker\mathbb{L}_{\kappa=0,h}$. Now, (94) tells that the discrete divergence of the velocity vanishes on the cells of a mesh of size $2\Delta x \times 2\Delta y$ with normal velocities on the edges of that mesh: see Fig. 7 (there are actually four overlapping such "Marker and Cell" meshes that cover the original mesh). It is easily checked that the space of velocities that verify (94) contains velocities that are such that there exists values $a, b, (\psi_{ij})$ such that

$$\forall (i,j) \in [1, N_x] \times [1, N_y] : u_{ij} = a + \frac{\psi_{ij+1} - \psi_{ij-1}}{2\Delta y} \quad \text{and} \quad v_{ij} = b - \frac{\psi_{i+1,j} - \psi_{i-1,j}}{2\Delta x}, \tag{95}$$

which means that the invariant set $\mathbf{u}_{ij}$ contains discrete curls and that this space is rich enough to discretize properly continuous divergence-free velocities. The fact that (95) is the only possible representation of velocities verifying (94) may be inferred from an adaptation of the works of Nicolaides [7] to the periodic cartesian case with odd N_x and N_y. Thus, in this case, we exactly have that $Ker\mathbb{L}_{\kappa=0,h} = \mathcal{E}_h^{\square}$. □

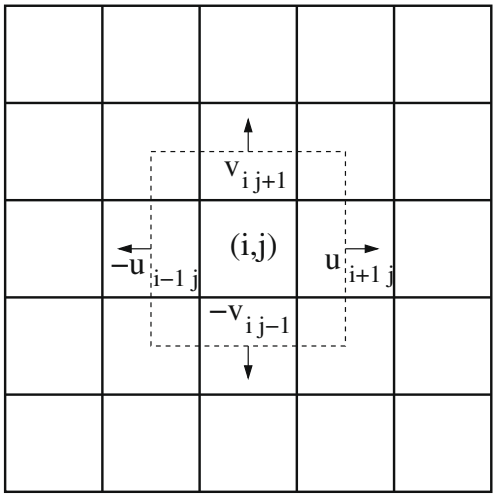

Fig. 7. MAC mesh of size $2\Delta x \times 2\Delta y$.

Appendix B. Proof of Lemma A.1

Let us suppose that $(\mathbf{u}_i)$ satisfies (91). By defining u_{ij} with $u_{ij} := \mathbf{u}_i \cdot \mathbf{n}_{ij}$ and by using the relation $\sum_{A_{ij} \subset \partial T_i} |A_{ij}| \mathbf{n}_{ij} = 0$ (which is valid for any type of mesh), we immediately obtain (92)(a). Moreover, (91) implies of course (92)(b). Let us now suppose that (92) is verified and let T_i be a non-degenerated triangle with three edges A_{ij_1}, A_{ij_2} and A_{ij_3}, and let $\mathbf{n}_{ij_1}, \mathbf{n}_{ij_2}$ and $\mathbf{n}_{ij_3}$ be the associated unit normal vectors exterior to T_i. Since the triangle T_i is non-degenerated, the system

$$\begin{cases} \mathbf{u}_i \cdot \mathbf{n}_{ij_1} = u_{ij_1}, \\ \mathbf{u}_i \cdot \mathbf{n}_{ij_2} = u_{ij_2} \end{cases}$$

allows to define a unique $\mathbf{u}_i$. Because of (92)(a), we have for this triangle T_i

$$|A_{ij_1}| \mathbf{u}_i \cdot \mathbf{n}_{ij_1} + |A_{ij_2}| \mathbf{u}_i \cdot \mathbf{n}_{ij_2} + |A_{ij_3}| u_{ij_3} = 0,$$

that is to say

$$\mathbf{u}_i \cdot (|A_{ij_1}| \mathbf{n}_{ij_1} + |A_{ij_2}| \mathbf{n}_{ij_2}) + |A_{ij_3}| u_{ij_3} = 0.$$

But, we know that we have for any type of mesh $\mathbf{u}_i \cdot \sum_{A_{ij} \subset \partial T_i} |A_{ij}| \mathbf{n}_{ij} = 0$. Thus, in our case, we have

$$|A_{ij_3}| (\mathbf{u}_i \cdot \mathbf{n}_{ij_3} - u_{ij_3}) = 0,$$

that is to say $\mathbf{u}_i \cdot \mathbf{n}_{ij_3} = u_{ij_3}$. Thus, for any $j \in \{j_1, j_2, j_3\}$, we have $\mathbf{u}_i \cdot \mathbf{n}_{ij} = u_{ij}$. Since this is true for any triangle T_i of the triangular mesh, we can construct $(\mathbf{u}_i)$ in such a way that $\mathbf{u}_i \cdot \mathbf{n}_{ij} = u_{ij}$ for any T_i. We conclude by noting that (92)(b) coupled to $\mathbf{u}_i \cdot \mathbf{n}_{ij} = u_{ij}$ implies that $\mathbf{u}_i \cdot \mathbf{n}_{ij} = -\mathbf{u}_j \cdot \mathbf{n}_{ji}$.

References

[1] P.L. Roe, Approximate Riemann solvers, parameter vectors and difference schemes, J. Comp. Phys. 43 (1981) 357–372.
[2] J.-M. Massella, I. Faille, T. Gallouët, On an approximate Godunov scheme, Int. J. Comput. Fluid. Dyn. 12 (1999) 133–149.
[3] T. Buffard, T. Gallouët, J.-M. Hérard, A sequel to a rough Godunov scheme: application to real gases, Comput. Fluids 29 (2000) 813–847.
[4] S. Clerc, Numerical simulation of the homogeneous equilibrium model for two-phase flow, J. Comp. Phys. 161 (2000) 354–375.
[5] M. Crouzeix, P.-A. Raviart, Conforming and nonconforming finite element methods for solving the stationary Stokes equations. I, Rev. Française Automat. Informat. Recherche Opérationnelle Sér. Rouge 7 (1973) 33–75.
[6] D.N. Arnold, R.S. Falk, A uniformly accurate finite element method for the Reissner–Mindlin plate, SIAM J. Numer. Anal. 26 (1989) 1276–1290.
[7] R.A. Nicolaides, Direct discretization of planar div-curl problems, SIAM J. Numer. Anal. 29 (1992) 32–56.
[8] R.A. Nicolaides, Analysis and convergence of the MAC scheme. I: The linear problem, SIAM J. Numer. Anal. 29 (1992) 1579–1591.
[9] S. Dellacherie, Analysis of Godunov type schemes applied to the compressible Euler system at low Mach number, J. Comp. Phys. 229 (4) (2010) 978–1016.
[10] H. Guillard, C. Viozat, On the behavior of upwind schemes in the low Mach number limit, Comput. Fluids 28 (1999) 63–86.
[11] H. Guillard, A. Murrone, On the behavior of upwind schemes in the low Mach number limit. II: Godunov type schemes, Comput. Fluids 33 (2004) 655–675.
[12] H. Guillard, A. Murrone, Behavior of upwind scheme in the low Mach number limit. III: Preconditioned dissipation for a five equation two phase model, Comput. Fluids 37 (10) (2008) 1209–1224.
[13] H. Guillard, On the behavior of upwind schemes in the low Mach number limit. IV: P0 approximation on triangular and tetrahedral cells, Comput. Fluids 38 (2009) 1969–1972.
[14] M.-S. Liou, A Sequel to AUSM: AUSM$^+$. Part II: AUSM$^+$-up for all speeds, J. Comp. Phys. 214 (1) (2006) 137–170.
[15] I. Mary, P. Sagaut, Large eddy simulation of flow around an airfoil near stall, AIAA J. 40 (6) (2002) 1139–1145.
[16] B. Thornber, D. Drikakis, Numerical dissipation of upwind schemes in low Mach flow, Int. J. Numer. Meth. Fluids 56 (2008) 1535–1541.
[17] B. Thornber, A. Mosedale, D. Drikakis, D. Youngs, R.J.R. Williams, An improved reconstruction method for compressible flows with low Mach number features, J. Comp. Phys. 227 (10) (2008) 4873–4894.
[18] X.-S. Li, C.-W. Gu, An all-speed Roe-type scheme and its asymptotic analysis of low Mach number behaviour, J. Comp. Phys. 227 (10) (2008) 5144–5159.
[19] X.-S. Li, C.-W. Gu, J.-Z. Xu, Development of Roe-type scheme for all-speed flows based on preconditioning method, Comput. Fluids 38 (2009) 810–817.
[20] S. Schochet, Fast singular limits of hyperbolic PDEs, J. Differ. Equ. 114 (1994) 476–512.
[21] F. Rieper, Influence of cell geometry on the behaviour of the first-order Roe scheme in the low Mach number regime, in: R. Eymard, J.-M. Hérard (Eds.), Proceedings of the Fifth Conference on Finite Volumes for Complex Applications, Wiley, 2008, pp. 625–632.
[22] F. Rieper, G. Bader, The influence of cell geometry on the accuracy of upwind schemes in the low Mach number regime, J. Comp. Phys. 228 (8) (2009) 2918–2933.
[23] S. Dellacherie, Checkerboard modes and wave equation, in: Proceedings of the Conference on Scientific Computing, Podbanske, Slovakia, 2009. pp. 71-80.
[24] R. Eymard, T. Gallouët, R. Herbin, Finite volume methods, in: P.G. Ciarlet, J.L. Lions (Eds.), Handbook of Numerical Analysis, vol. 7, North-Holland/Elsevier, Amsterdam, 2000, pp. 713–1020.
[25] B. Perthame, Boltzmann type schemes for gas dynamics and the entropy property, SIAM J. Num. Anal. 27 (1990) 1405–1421.
[26] F.H. Harlow, J.E. Welch, Numerical calculation of time-dependent viscous incompressible flow of fluid with free surface, Phys. Fluids 8 (12) (1965) 2182–2189.
[27] R.D. Richtmyer, K.W. Morton, Difference Methods for Initial-Value Problems, Krieger, second ed., 1994.